Jammerland Bay Nearshore A/S

Hydrography and sediment spill

JANUARY 2017

Jammerland Bay Nearshore A/S

Hydrography and sediment spill

JANUARY 2017

Client	Jammerland Bay Nearshore A/S Gyngemose Parkvej 50 2860 Søborg
Consultant	Orbicon A/S Ringstedvej 20 DK-4000 Roskilde
Sub-consultant	Royal HaskoningDHV Rightwell House, Bretton Peterborough, PE3 8DW United Kingdom
Project no.	3621400172
Document no.	JB-TR-006
Project manager	Kristian Nehring Madsen
Prepared by	DR. David S. Brew, Anh Le, Dai Luong, DR. Keming Hu
Reviewed by	Dr. Nick Cooper
Version no.	02
Approved by	Kristian Nehring Madsen
Published	January 2017

TABLE OF CONTENT

SUMMARY

This report provides an assessment of the potential impacts of the proposed Jammerland Bight offshore wind farm development on hydrography (tidal current velocity and direction) and sediment spill. In order to assess the potential impacts of the wind farm (including all associated infrastructure) and the export cable corridor, relative to baseline (existing) conditions, detailed numerical modelling has been employed. These impacts have been assessed using a set of worst case characteristics developed through experience of previous wind farms in this sector of the North Sea, particularly Horns Rev 3 (Energinet.dk, 2014). Considerations of the proposed impacts upon the tidal current and sediment transport regimes have been made for the construction, operation and decommissioning phases of the development.

Pressures during Construction

Over the period of construction there is the likelihood for discrete short-term disturbances of the offshore seabed as the wind turbine foundations and the export and inter-array cables are installed sequentially across the development site. Seabed sediments have the potential to be released into the water column resulting in the formation and distribution of sediment plumes.

In this assessment, the worst case scenario regarding sediment spill and transport was considered to be seabed preparation for concrete GBS foundations and jetting for inter-array and export cable installation. A worst case total of nine foundations in three blocks were assumed to be installed synchronously followed by the laying of six inter-array cables per block. In the modelled worst case scenario, foundations were located at the northwest, northeast and southern extremes of the potential development area to provide an indication of the worst geographical spread of sediment released into the water column.

The results show that the worst case sediment plume for the foundations and inter-array cables attains predicted suspended sediment concentrations of less than 50mg/l with isolated patches (less than 500m diameter) over 90mg/l over a 30-day simulation period. Concentrations reduce to zero within 350m of the foundations and cable transects in all directions. Suspended sediment concentrations predicted to be greater than 10mg/l are only exceeded up to 1% of the simulation period. Maximum bed thickness change (sediment deposition from the plume) throughout the 30-day simulation period was predicted to be about 20mm along the routes of the cables, decreasing to zero less than 250m from the cables.

The effect on sediment transport of jetting the export cable was modelled over a 2-day simulation period. Along the export cable, the suspended sediment concentration was predicted to increase from less than 10mg/l in the bottom layer near the development area to a patch over 90mg/l near the coast. The concentration reduces to zero up to 300m to the northwest and southeast of the cable. In the middle and surface layers,

concentrations are predicted to be effectively zero along more than half of the seaward part of the cable increasing to 40mg/l (middle layer) and 30mg/l (surface layer) near the coast. Suspended sediment concentrations greater than 10mg/l are only exceeded up to 2% of the simulation period. Maximum bed thickness change throughout the simulation period was predicted to be less than 9mm local to the cable route, decreasing to zero up to 200m away to either side.

Pressures during Operation

The greatest potential for changes in the tidal current regime occurs during the operational phase of the wind farm. In this assessment, the effect of operation on these processes was modelled using a worst case layout of 3MW foundations across the proposed development area. No potential effects are considered for the inter-array and export cables because, during operation, they are assumed to be buried.

The results show predicted changes to tidal currents would be relatively small. The maximum change to current velocities in the surface, middle and upper layers of the water column is predicted to be +/-0.006m/s. The predicted changes in tidal current velocities are so small that they would not translate into changes to sediment transport pathways and morphology.

Pressures during Decommissioning

The decommissioning phase is generally considered to incur similar or lesser changes to tidal currents and sediment spill and transport than the construction phase.

Impact Assessment

The table below describes the impact significance for the environmental factors related to hydrography and sediment spill during construction, operation and decommissioning of the wind farm.

Phase	Environmental Factor	Impact Significance
Construction	Suspended sediment concentrations and deposition (foundations and cables)	Negligible Negative
	Natura 2000 sites	No Impact
Operation	Changes to tidal currents (foundations)	No Impact
	Natura 2000 sites	No Impact
Decommissioning	Suspended sediment concentrations and deposition (foundations and cables)	Negligible Negative
	Natura 2000 sites	No Impact

1. INTRODUCTION

1.1. Jammerland Bight Offshore Wind Farm

The proposed Jammerland Bight offshore wind farm is located in a shallow water area (Jammerland Bight in the Great Belt) in the western Baltic Sea (Figure 1.1). The area outlined for development occupies approximately 65km^2 about 4km southwest of Sjælland Island. Jammerland Bay Nearshore A/S (the developer) has agreed with the Danish Energy Agency for a target capacity of 240 Megawatt (MW) for Jammerland Bight offshore wind farm.

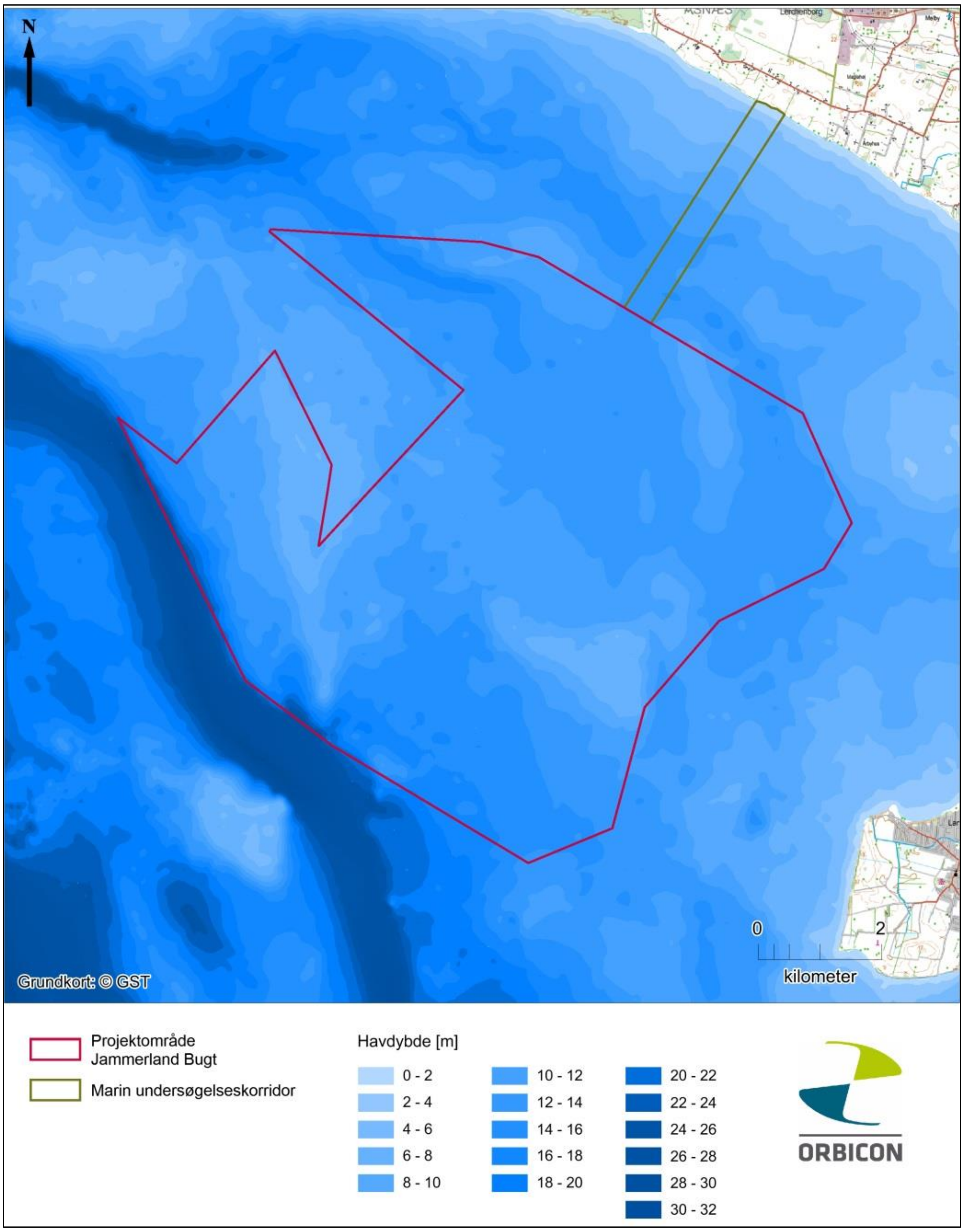

Figure 1.1 Location of the proposed Jammerland Bight offshore wind farm and the proposed export cable corridor towards the landfall at Østrup on Sjælland Island.

Electricity from Jammerland Bight will be transferred to shore by an export cable, which will be routed to a landfall site at Østrup on the island of Sjælland (Figure 1.1). An export cable corridor has been delineated which is 500m wide, stretching from the proposed wind farm to shore, with the flexibility to place the cable anywhere within the corridor. The corridor exits from the northeast side of the wind farm development area and is approximately 4km long from its offshore connection to the beach at Østrup.

1.2. Objectives

This report provides an assessment of the potential changes to prevailing tidal current and sediment transport conditions arising as a result of the construction, operation and decommissioning of Jammerland Bight. The assessment of effects, in turn, informs the assessment of direct and indirect impacts on a range of parameters (e.g. benthic ecology, fisheries) that will be studied as separate parts of the EIA process.

This report presents an understanding of the existing tidal and sediment transport processes across the Jammerland Bight development area and the associated export cable corridor. This is followed by the definition of worst case scenarios for each element of the development in terms of their potential effects on hydrography and sediment spill, which are then compared to the existing conditions through numerical modelling.

The potential effects have been assessed conservatively using worst case characteristics for the proposed Jammerland Bight project. This is because the specific details of the project have not been resolved and there are still a number of alternatives available in the choice of, for example, turbine type, foundation type and layout, prior to application. The use of worst case is an acknowledged EIA approach where the details of the whole project are not available when the application is submitted. The worst case scenario for each individual impact is used so that it can be safely assumed that all lesser options will have less potential impact.

1.3. Project Description

The key components of the Jammerland Bight offshore wind farm development, in the context of potential effects on hydrography and sediment spill, are the type and size of foundations and their layout pattern, and the installation methodologies for the foundations, export and inter-array cables.

1.3.1 Foundation Type and Layout

A range of different foundation types and sizes could be combined to create the 240MW capacity for Jammerland Bight. Jammerland Bay Nearshore A/S is considering two wind turbine sizes and layouts:

- a minimum wind turbine size of 3MW of which 80 foundations would be installed to reach a capacity of 240MW; and
- a 7MW wind turbine where 35 foundations would approximately 240MW of power.

The 3MW and 7MW wind turbines are the minimum and maximum sizes being considered so that any turbine between these two sizes will be covered by the impact assessment. The proposed 3MW and 7MW layouts are shown in Figure 1.2.

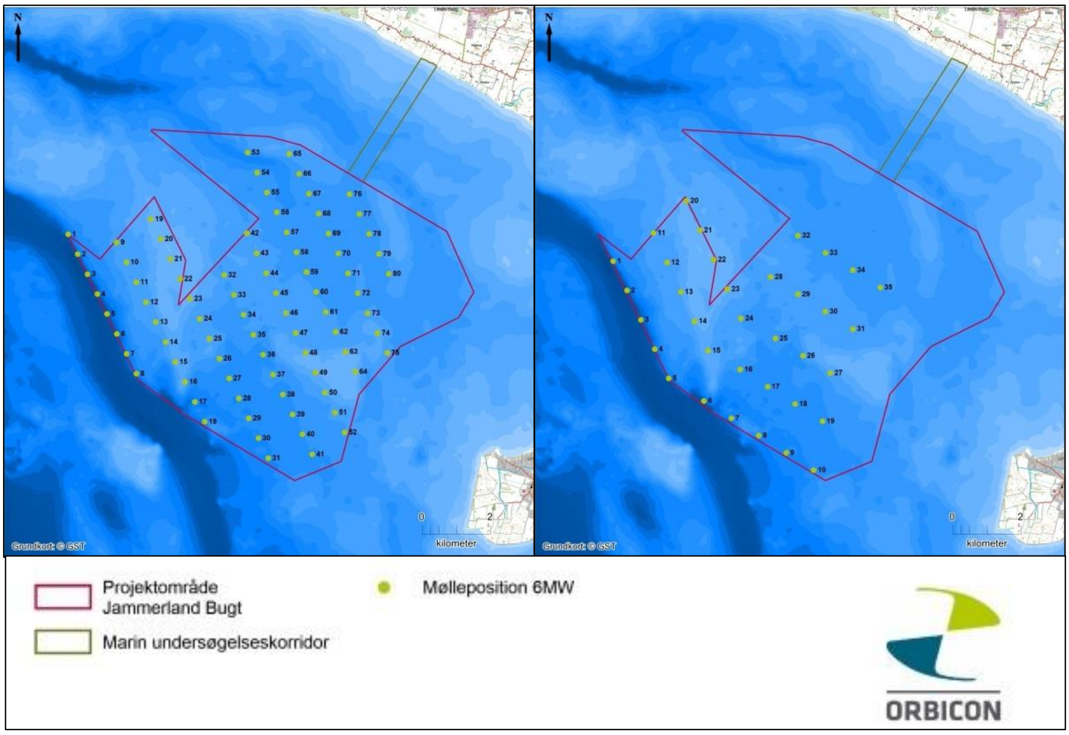

Figure 1.2 Layouts for 3MW (left) and 7MW (right) wind turbine foundations across the development area.

1.3.2 Installation of Foundations

The greatest effect on hydrography during the construction phase of the development will depend on the installation method used; different installation methods are required for different foundation types. Conical GBS foundations rely on their mass including ballast to withstand the loads generated by the offshore environment and the wind turbine. For GBS foundations, an area of seabed may need to be dredged in order to provide a levelled surface upon which they are installed. No seabed preparation is necessary for any other foundation type; however, jackets may need pre-dredging prior to piling for each jacket leg.

1.3.3 Installation of Cables

The Jammerland Bight export cable and inter-array cables are assumed to be installed using jetting. Jetting works by fluidising the seabed using a combination of high-flow, low pressure and low flow, high pressure water jets to cut into sands, gravels and low to medium strength clays. The jetting is assumed to take place from the landfall and seawards.

1.4. Potential Impacts during Construction

During the construction phase of the proposed Jammerland Bight offshore wind farm, there is potential for foundation and cable installation activities to cause water and sediment disturbance, potentially resulting in changes in suspended sediment concentrations and/or seabed levels due to deposition or erosion. These potential impacts include:

- changes in suspended sediment concentrations due to foundation and inter-array cable installation;
- changes in seabed levels due to foundation and inter-array cable installation;
- changes in suspended sediment concentrations due to export cable installation; and
- changes in seabed levels due to export cable installation.

1.5. Potential Impacts during Operation

During the operational phase of the proposed Jammerland Bight offshore wind farm, there is potential for the presence of the foundations to cause changes to the tidal regime due to physical blockage effects.

1.6. Potential Impacts during Decommissioning

The types of effect during decommissioning will be comparable to those identified for the construction phase:

- changes in suspended sediment concentrations due to foundation and inter-array cable removal;
- changes in seabed levels due to foundation and inter-array cable removal;
- changes in suspended sediment concentrations due to export cable removal; and
- changes in seabed levels due to export cable removal.

1.7. Environmental Designations

The proposed Jammerland Bight offshore wind farm is located between five protected marine sites (Figure 1.3). These are the Baltic Sea Protected Areas (HELCOM):

- Central Great Belt and Vresen (368km^2 located south of the development – 116 on Figure 1.3);
- The Sea between Romsø and Hindsholm and Romsø (43km^2 located south-west of the development - 109);
- Fyns Hoved, Lillegrund og Lillestrand (22km^2 located west of the development - 107);
- Ryggen (4km^2 located west of the development - 196) and;
- Røsnæs, Røsnæs Rev og Kalundborg Fjord (57km^2 located north of the development - 166).

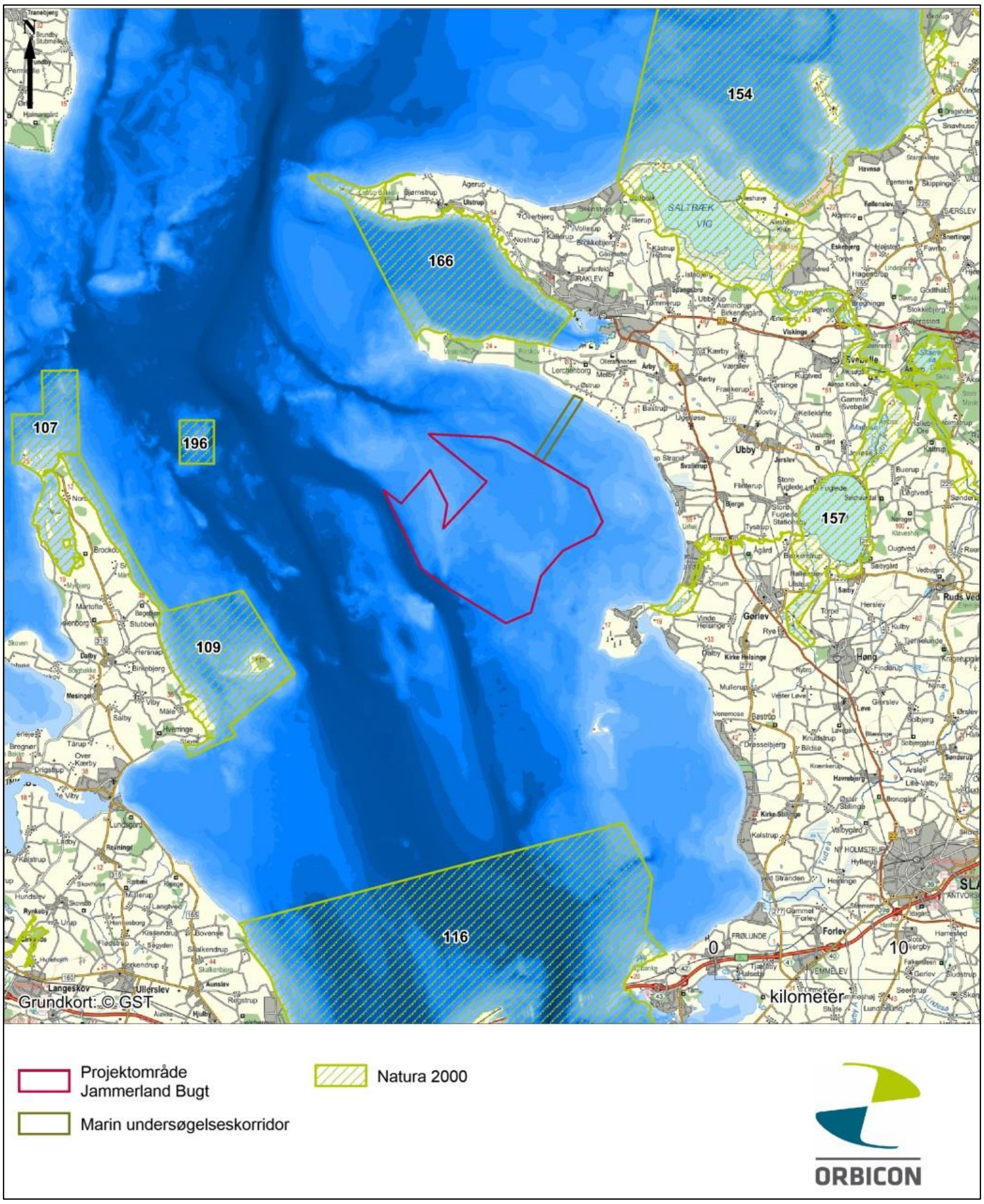

Figure 1.3 Marine Protected Areas nearest to Jammerland Bight offshore wind farm.

1.8. Assessment Methodology

To ensure a uniform and transparent basis for the EIA, a general methodology for the assessment of predicted impacts has been prepared together with a list of terminology (Figure 1.4). In this method the overall goal is to describe the Severity of Impact caused by Jammerland Bight offshore wind farm. The assessment begins with two steps; to define the magnitude of the pressure and the sensitivity of the environmental factor, the combination of which gives the Degree of Impact, which, in turn is combined with the importance to give the Severity of Impact. It may be necessary to consider the risk of a certain impact occurring, and in these cases, the Severity of Impact is considered against the Likelihood of the occurrence, giving the Degree of Risk.

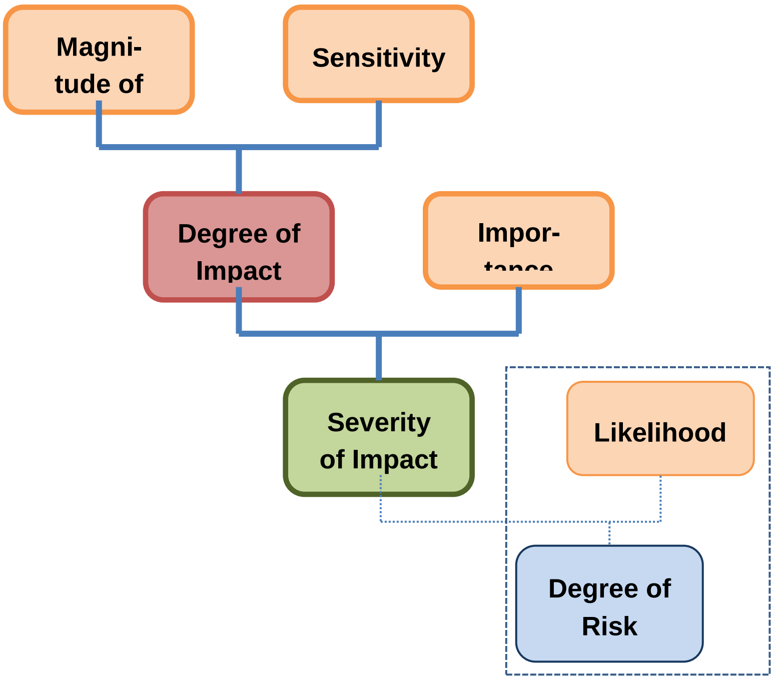

Figure 1.4. Generic methodology used for impact assessment of Jammerland Bight offshore wind farm.

1.8.1 Magnitude of Pressure

The methodology adopted to understand changes to hydrography caused by Jammerland Bight is initially taken to the level of Magnitude of Pressure (Figure 1.4). The magnitude of pressure is defined by pressure indicators (Table 1.1). These indicators are based on the effects on hydrography and sediment spill in order to achieve the most optimal description of pressure; for example; millimeters of sediment deposited within a certain period and area in excess of natural deposition values. The magnitude of pressure is defined as low, medium, high or very high and is defined by its duration and range (spatial extent) (Table 1.1).

Table 1.1. Definition of the magnitude of pressure.

Magnitude	Duration	Range
Very High	Recovery takes longer than ten years or is permanent	International
High	Recovered within ten years after end of construction	National
Medium	Recovered within five years after end of construction	Regional
Low	Recovered within two years after end of construction	Local

1.8.2 Sensitivity

Sensitivity to a pressure varies between environmental factors. For hydrography and sediment spill, the sensitivity of the receptor is a function of its capacity to accommodate change and reflects its ability to recover if it is affected. Table 1.2 sets out the generic criteria used to define the sensitivity of the physical marine environment to change.

Table 1.2. Criteria to determine the sensitivity of the marine environment to change.

Sensitivity	Criteria
Very High	The marine environment has a very low capacity to accommodate any change to hydrography and/or sediment spill, compared to baseline conditions
High	The marine environment has a low capacity to accommodate any change to hydrography and/or sediment spill compared to baseline conditions
Medium	The marine environment has a high capacity to accommodate changes to hydrography and/or sediment spill due, for example to, large size of water body, location away from sensitive habitats and a high capacity for dilution. Small changes to baseline conditions are, however, likely
Low	Physical conditions are such that they are likely to tolerate proposed changes with little or no impact on baseline conditions

1.8.3 Degree of Impact

Jammerland Bight has a large physical scale and a high degree of temporal and spatial variance for all hydrographical and sediment spill parameters considered. As a result, the marine environment in relation to hydrography and sediment spill is considered to be of medium sensitivity. In order to determine the degree of impact; the magnitude of pressure and sensitivity are combined in a matrix (Table 1.3). The degree of impact is the description of an impact to a given environmental factor without putting it into a broader perspective (the latter is acheived by including importance in the evaluation, Table 1.4).

Table 1.3. Matrix for the assessment of the degree of impact.

Magnitude of Pressure	Sensitivity			
	Very High	High	Medium	Low
Very High	Very High	Very High	High	High
High	Very High	High	High	Medium
Medium	High	High	Medium	Low
Low	Medium	Medium	Low	Low

1.8.4 Importance

The importance of the environmental factor is assessed for each environmental sub-factor. Some sub-factors are assessed as a whole, but in most cases, the importance assessment is broken down into components and/or sub-components in order to conduct an environmental impact assessment. The importance criteria are graded into four tiers (Table 1.4).

Table 1.4. Definition of importance to an environmental component.

Importance Level	Description
Very High	Components protected by international legislation/conventions (Annex I, II and IV of the Habitats Directive, Annex I of the Birds Directive), or of international ecological importance. Components of critical importance for wider ecosystem functions
High	Components protected by national or local legislation, or adapted on national “Red Lists”. Components of importance for far-reaching ecosystem functions
Medium	Components with specific value for the region, and of importance for local ecosystem functions
Low	Other components of no special value, or of negative value

1.8.5 Severity of Impact

The severity of impact is assessed from the grading of the degree of impact and importance of the environmental factor, using the matrix shown in Table 1.5. If it is not possible to grade the degree of impact and/or importance, an assessment is given based on expert judgement.

Table 1.5. Matrix for the assessment of the severity of impact.

Degree of Impact	Importance of the Environmental Component			
	Very High	High	Medium	Low
Very High	Very High	High	Medium	Low
High	High	High	Medium	Low
Medium	Medium	Medium	Medium	Low
Low	Low	Low	Low	Low

1.8.6 Significance of Impact

Based on the severity of impact, the significance of the impact can be determined through the phrases described in Table 1.6.

Table 1.6. Definition of significance of impact.

Severity of Impact	Significance of Impact	Dominant Effects
Very High	Significant Negative	Impacts are large in extent and/or duration. Recurrence or likelihood is high, and irreversible impacts are possible
High	Moderate Negative	Impacts occur, which are either relatively large in extent or are long term in nature (lifetime of the project). The occurrence is recurring, or the likelihood for recurrence is relatively high. Irreversible impact may occur, but will be strictly local, on, for example, cultural or natural conservation heritage
Medium	Minor Negative	Impacts occur, which may have a certain extent or complexity. Duration is longer than short term. There is some likelihood of an occurrence but a high likelihood that the impacts are reversible
Low	Negligible Negative	Small impacts occur, which are only local, uncomplicated, short term or without long term effects, and without irreversible effects
Low	Neutral / No Impact	No impact compared to status quo
	Positive Impacts	Positive impact occurring in one or more of the above statements

2. TIDAL CURRENTS AND SEDIMENTARY PROCESSES

2.1. Data Collection

Metocean data including water levels, tidal currents, salinity and temperature, and wind and air pressure data, and bathymetry has been collated from a variety of sources and located in the Baltic Sea near the Danish coastline (Table 2.1).

Table 2.1. Baseline data collected for Jammerland Bight offshore wind farm.

Location	Data Type	Period	
		Start	End
Baltic Sea	Modelled wind and air pressure (SKA model of DMI)	October 2013	October 2014
Ten coastal tide gauges	Measured water levels	October 2013	June 2014
One current meter	Measured tidal current velocities	October 2013	June 2014
Ten selected offshore locations	Modelled water levels, vertical profile of tidal currents, salinities and temperatures (DMI model)	October 2013	June 2014

2.1.1 Conventions and Definitions

All directions are given in nautical convention. This means that for wind the direction refers to the direction where the wind is coming from and measured positive in degrees from true north; for tidal currents the direction refers to the direction where the tidal currents are going to and measured positive in degrees from true north.

2.2. Modelled Wind and Air Pressure

A one-year dataset of spatial wind from the SKA model of DMI was generated to cover the Baltic Sea and the eastern North Sea. The wind data has a 3km resolution and was extracted at hourly time intervals between 1st October 2013 and 31st October 2014.

Low wind speeds occur in summer time (April to July) while strong winds occur in winter time (November to January). The average wind speed is about 4-8m/s during normal conditions. The wind data also covers the storm event which occurred on 5-6th December 2013 where wind speed increased up to 30m/s (Figure 2.1). The associated air pressure is shown in Figure 2.2.

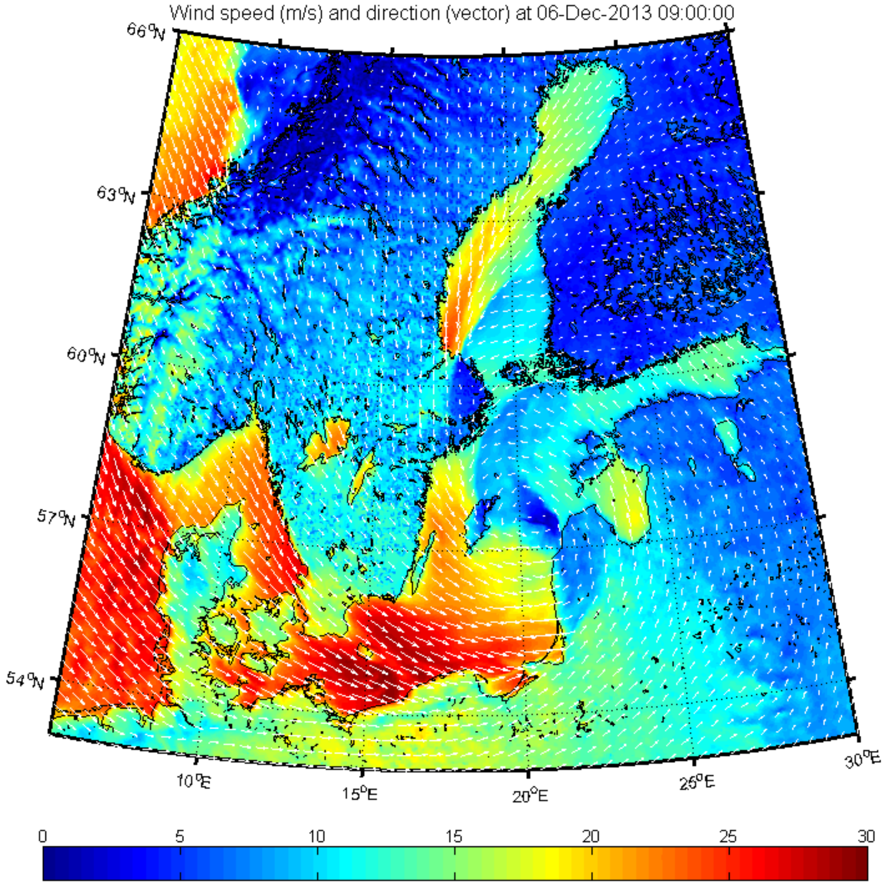

Figure 2.1. Wind speed in the Baltic Sea during cyclone Xaver (9:00am on 6th December 2013).

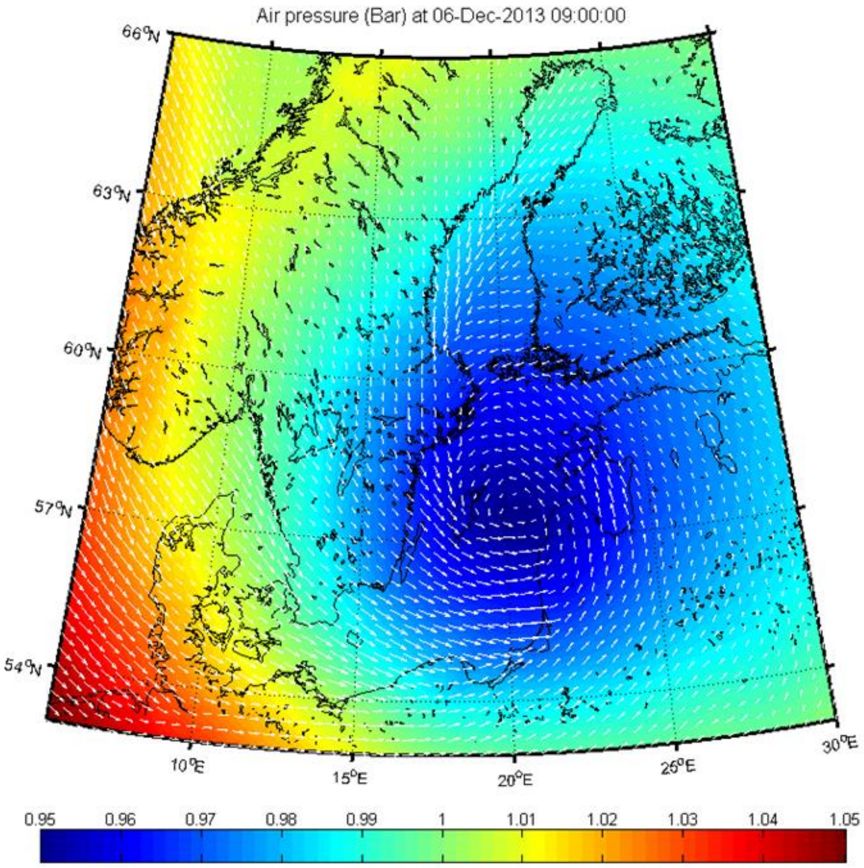

Figure 2.2. Air pressure in the Baltic Sea during cyclone Xaver (9:00am on 6th December 2013).

2.3. Measured Water Levels

Measured water levels relative to Danish Vertical Reference 1990 (DVR90 which is approximately mean sea level) between October 2013 and June 2014 were collated at ten coastal locations along the Danish Baltic Sea coast (Figure 2.3). All the recording stations are located inside ports, and so the characteristics of the water levels may be influenced by local bathymetry and geomorphology. The tidal range in the western Baltic Sea is small, varying from 0.6m in the Kattegat to 0.2-0.4m south of the Langelandsbælt Belt. The measured water level data were used to calibrate the regional model.

2.4. Storm Event on 5-6th December 2013

The northwest Atlantic Ocean experienced a rare storm on 5-6th December. During the event, the North Sea, Kattegat and Baltic Sea all received large surges. The UK Environment Agency claimed it was “the biggest UK storm surge for 60 years”. In the Kattegat, the peak water level recorded at Hornbak on 6th December 2013 was 1.9m (above DVR90 datum) which exceeded the estimated 1 in 100 year water level of 1.68m provided by the Danish Coastal Authority.

Figure 2.3. Stations where water levels (yellow pins) and tidal current velocities (red dots) were measured.

2.5. Measured Tidal Currents

Multi-depth velocity measurements from current meters were available from October 2013 to June 2014 at three locations: Østerrenden, Vengeancegrund and Drogden (Figure 2.3). At Drogden, tidal current velocities were recorded at water depths of 3m, 5m and 10m but it is outside the domain of the 3D model and was not used. The current data at Vengeancegrund is limited due to a technical error and was also not used.

Current velocities at Østerrenden, close to the development area, were recorded at depths of 5m, 10m and 14m. At this location, the current velocities vary from 0.2m/s to 0.6m/s under normal conditions but can increase to 1.6m/s during storms. The measured tidal current data were used to calibrate the local model.

2.6. Modelled Data

DMI operates a regional 3D ocean model HBM for the North Sea and Baltic, in order to provide information about the physical state of the Danish and nearby waters in the near future. The HBM was developed in the early 1990's at Bundesamt für Seeschifffahrt und Hydrographie (BSH) in Hamburg, Germany. At the time, the model was known as BSHcmod. It has undergone extensive revision when it was implemented by DMI with co-operation between DMI, BSH, and other Baltic institutes.

HBM modelled data are available at ten locations (Figure 2.4). The data at each location comprises water levels and vertical profiles of tidal currents, salinities and temperatures. The data were extracted from the model every ten minutes between October 2013 and June 2014.

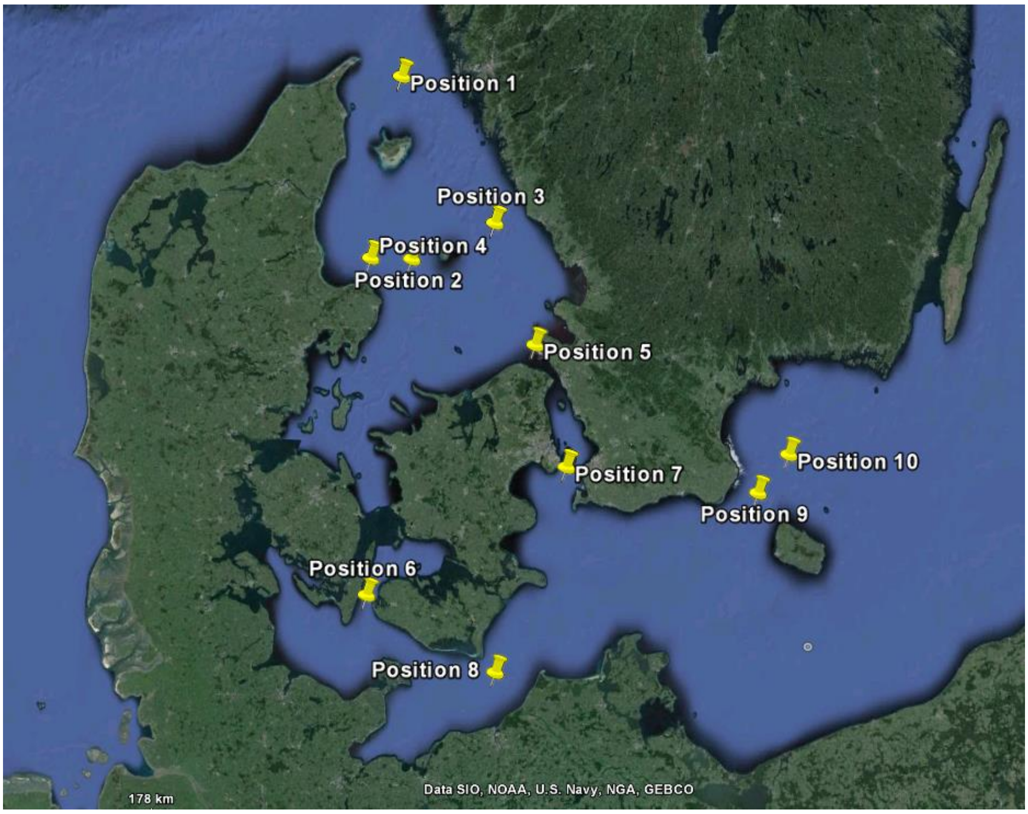

Figure 2.4. Stations where modelled water levels, tidal currents, salinities and temperatures were extracted.

2.6.1 Modelled Tidal Currents

The modelled current data were extracted for layers from the sea surface to the sea-bed. Along the vertical profile, the layer thickness towards the top of the water column was 2m reducing to 1m through the lower layers. The number of vertical layers varied from location to location due to different water depths. The modelled current data was used to calibrate the local model.

A surface tidal current rose at Position 6 (in Langelandsbælt Belt closest to the development) derived from the model is shown in Figure 2.5. The rose shows the flows are dominantly oriented north and south with peak current velocities greater than 2m/s. Calm periods (less than 0.1m/s) occur approximately half of the time.

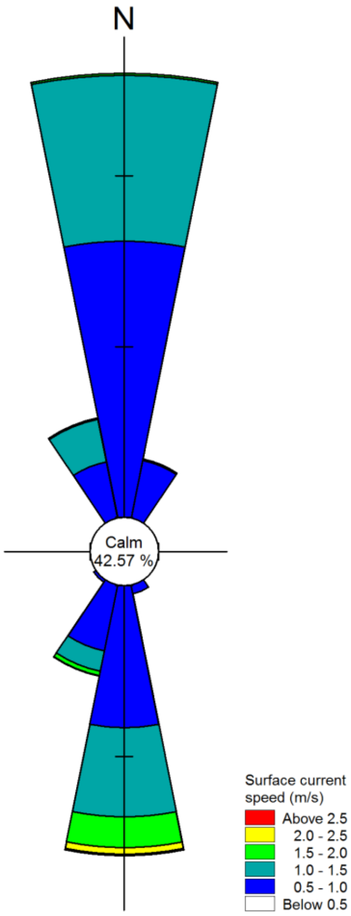

Figure 2.5. Surface tidal current distribution at Position 6 in Langelandsbælt Belt. Location is shown in Figure 2.4.

2.6.2 Modelled Salinities and Temperatures

Salinities and temperatures in the surface layer, middle layer and bottom layer during winter (December to February) are presented here from the Kattegat and the area of the Baltic Sea south of Lolland-Falster Islands (Figures 2.6 and 2.7). Although the water temperatures at all locations range from 5ºC to 10ºC, there are significant differences in salinity between the two chosen locations. The salinity in the Kattegat has the highest salinity in the bottom water and the lowest in the surface water. This highest salinity water ranges from 20 to 32PSU. This area has a very strong vertical stratification except in December. During December, due to the influence of storms, the currents are well mixed, resulting in weak salinity stratification.

The salinities south of the Lolland-Falster Islands are 8-18PSU, influenced by low salinity inflow from the brackish Baltic Sea. The sea water is unstratified in the winter. The wind farm is located in the Storebælt (Great Belt) between these two locations, but closer to the low salinity of the southern modelled point. Low salinity surface water from the Baltic Sea drains into the Kattegat through the Danish straits, and therefore, the wind farm location is likely to be influenced by this low salinity flow.

Figure 2.6. Selected salinity and temperature stations (results shown on Figure 2.7).

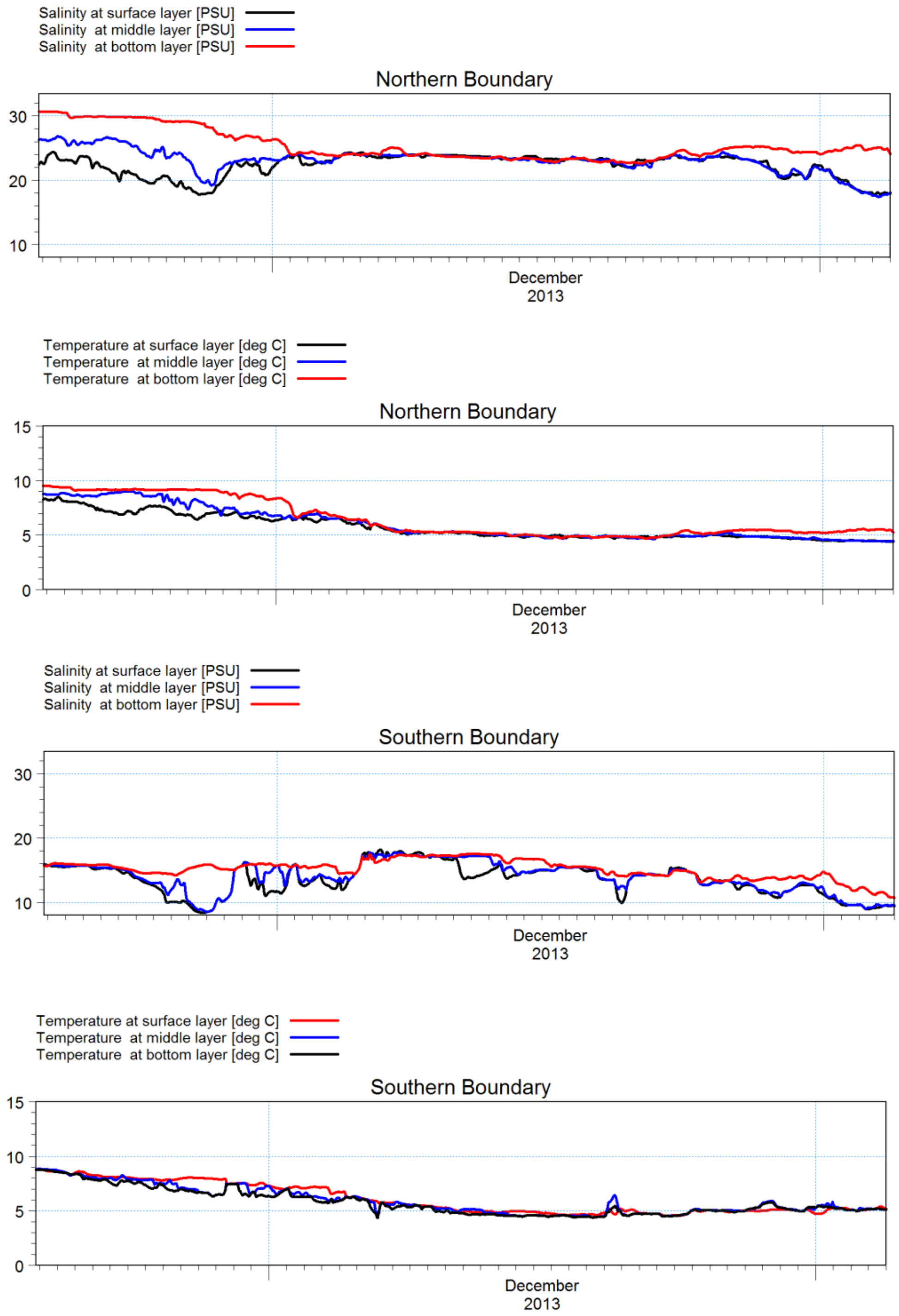

Figure 2.7. Salinity and temperature data extracted from the DMI model (stations shown on Figure 2.6; northern boundary refers to Kattegat and southern boundary refers to area of sea south of Lolland-Falster Islands).

2.7. Bathymetry

The bathymetry has been obtained from three sources (Figure 2.8):

- detailed bathymetric survey covering Jammerland Bight offshore wind farm;
- detailed bathymetric survey covering the adjacent straits; and
- C-map data covering a large area extending from the Baltic Sea to the North Sea.

The majority of bathymetry data is extracted from the global Electronic Chart Database (C-Map database) of Jeppesen Norway. These data are referenced to chart datum (CD). The surveyed bathymetric data are collected in two areas; the wind farm at Jammerland Bight and the wider Great Belt area. The bathymetric data at the wind farm is high resolution (50m). For the survey data, the datum was referenced to DVR90 (approximately mean sea level). All input depths are converted to UTM zone 32, datum WGS 84, in relation to approximately mean sea level. The areas covered by the more detailed survey data at Jammerland Bight are shown in Figure 2.9.

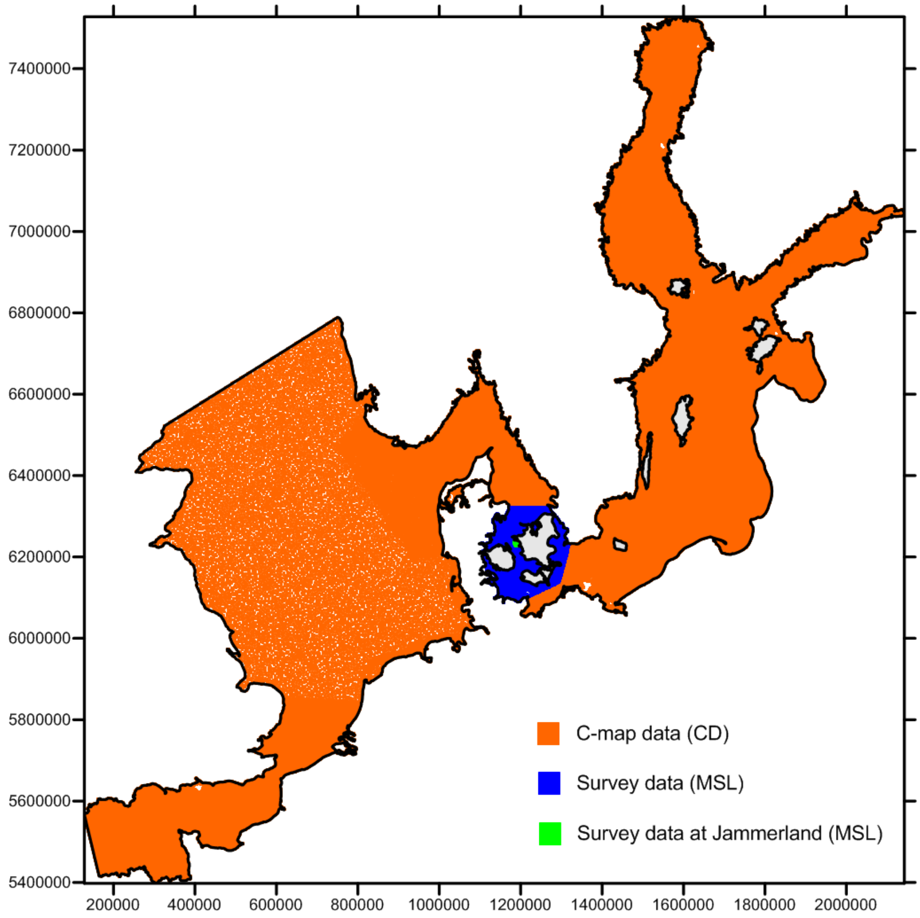

Figure 2.8. Sources of bathymetric data.

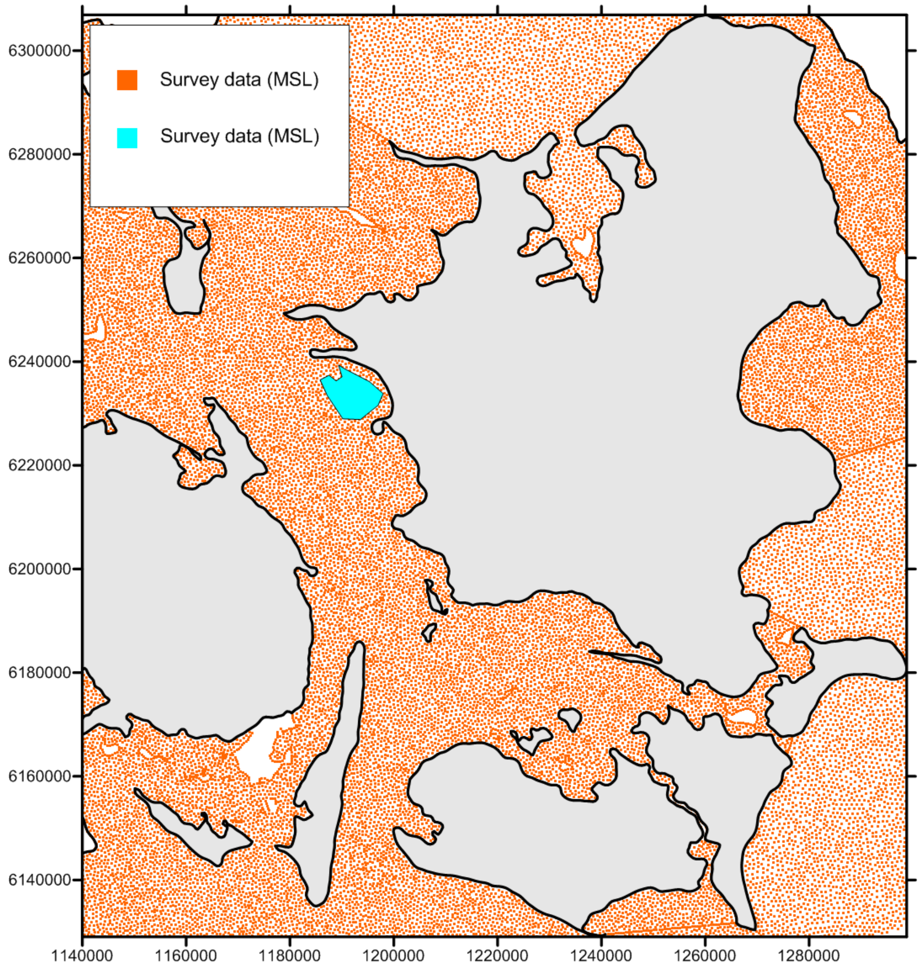

Figure 2.9. Survey data at Jammerland Bight (light blue) and the adjacent straits (orange).

The water depths across Jammerland Bight range from -8m to -24m mean sea level. The western fringe is in deeper water and the seabed slope is much steeper there compared to the eastern area (Figure 2.10).

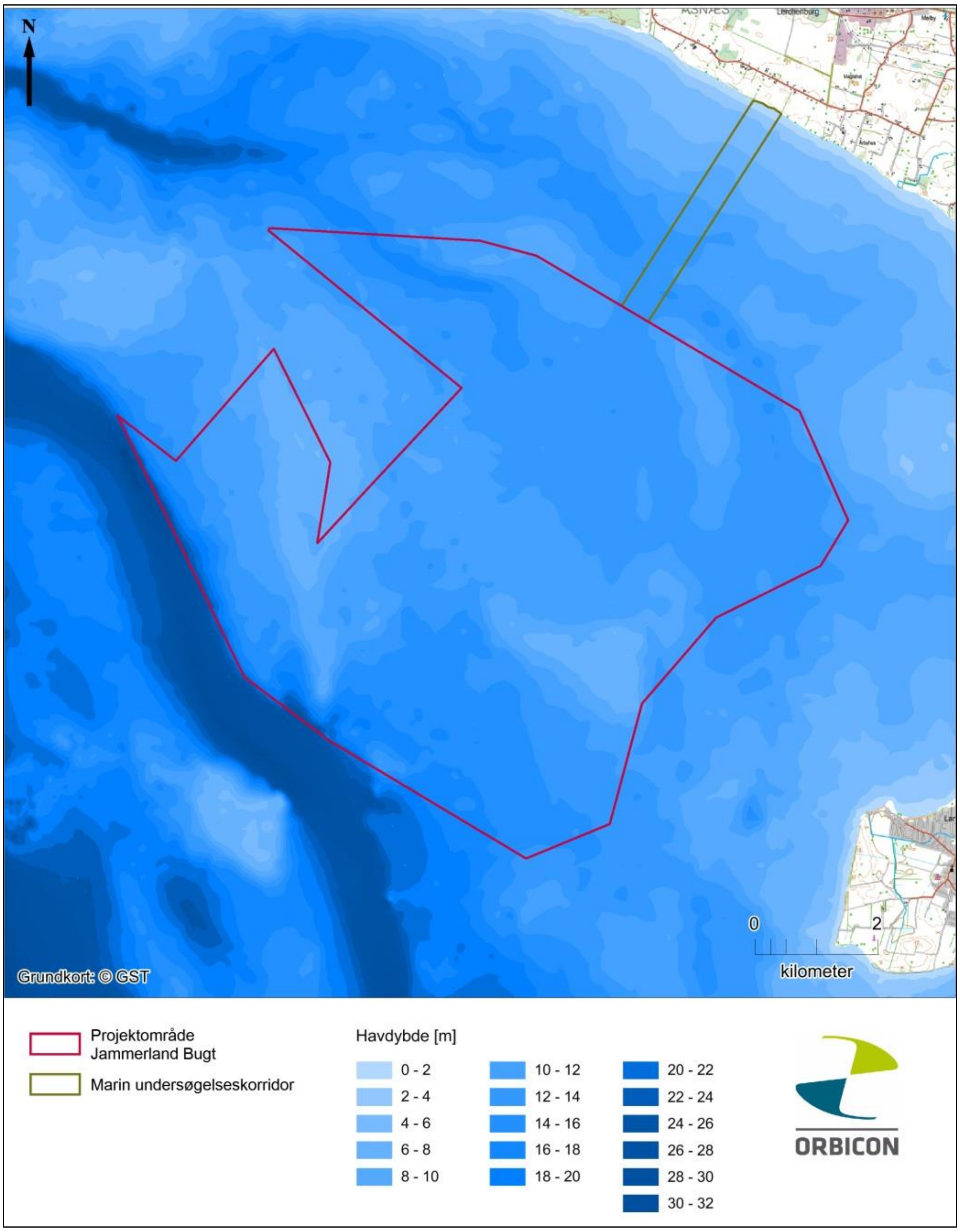

Figure 2.10. Bathymetry within the proposed Jammerland Bight offshore wind farm and adjacent areas.

2.8. Seabed Sediment Distribution

Jammerland Bay Nearshore A/S has supplied six seabed sediment samples across Jammerland Bight; five located in the development area and one at the seaward end of the export cable corridor (Figure 2.11). All of the recovered samples have been analysed for particle size distribution.

Figure 2.11. Location of grab samples for Jammerland Bight offshore wind farm.

Particle size data from the six seabed sediment sample sites are summarised in Table 2.2. They describe variable particle sizes across the development area. The proportions of mud are highest in sample 14586 (72%) and sample 14588 (78%) in the central and southwest parts of the development area, respectively. At the other end of the particle size spectrum, samples 14587 (southeast) and 14589 (northwest) contain less than 1% mud. Intermediate volumes of mud occur in sample 14584 (14%) and sample 14585 (33%) in the north part of the development area and at the seaward end of the export cable, respectively.

Table 2.2. Particle size distribution of seabed sediment samples across the development area locations are shown on Figure 2.11).

Sample ID	Location	% mud	% sand	% gravel
		<0.063mm	0.063mm-2mm	>2mm
14584	North	14.33	85.54	0.13
14585	Export Cable	32.75	67.13	0.12
14586	Central	72.42	25.89	1.69
14587	Southeast	0.82	66.20	32.98
14588	Southwest	78.04	20.94	1.02
14589	Northwest	0.33	96.09	3.58

3. WORST CASE SCENARIOS

The hydrography and sediment spill effects are predicted by comparing the existing environmental conditions with the worst case conditions created by the construction, operation and decommissioning of Jammerland Bight. Several numerical modelling tools have been used to support the assessment of existing conditions and the potential effects of the proposed wind farm and cables on hydrography and sediment spill.

The worst case characteristics of Jammerland Bight in terms of its effects on hydrography and sediment spill are adopted. The GBS represent the worst case foundations, in terms of physical blockage to tidal currents. There is now a considerable evidence base across the offshore windfarm industry which indicates that the greatest potential effect is associated with conical gravity base structures (Forewind, 2013). This is because these structures occupy a significant proportion of the water column as a solid mass (as opposed to an open lattice of slender columns and cross-members, like for example jackets or tripods, or a single slender column like a monopile). They do, therefore, have the potential to affect near-surface tidal currents in a manner that other foundation types do not.

Hence, the conical GBS foundation has been incorporated in the numerical modelling of operational effects on these physical processes elements for Jammerland Bight. Should other foundation types ultimately be selected following the design optimisation of the development, then the effects on tidal currents will be less than those presented for the worst case GBS.

Two potential worst case gridded layouts for Jammerland Bight have been considered to determine the worst case for hydrography and sediment spill. These are layouts filled entirely with 3MW or 7MW GBS foundations (Figure 1.2). The layout composed entirely of 3MW GBS foundations represents the smallest foundation type with a relatively narrow spacing, whereas the layout composed entirely of 7MW foundations represents the largest foundation type with a relatively wide spacing.

For the purpose of predicting effects on tidal currents and sediment transport, the worst case scenario is considered to be a layout composed on 3MW foundations (Figure 1.2 left panel). This provides the layout with the maximum potential for interaction of tidal current processes because the spacing is the narrowest, inducing the largest potential blockage.

3.1. Worst Case Construction Process and Assumptions for Foundations and Inter-array Cables

Increases in suspended sediment concentration may result from disturbance arising from construction activities. In order to define the worst case scenario for foundation installation and inter-array cable laying a conservative approach was adopted. In this approach, three sets of nine conical GBS foundations distributed across the northwest, northeast and southern sides of the development area and a set of inter-array cables connecting them (Figure 3.1), were installed over a 27-day period and simulated over a 30-day period. The locations of the three sets of foundations have been chosen to capture differences in sediment particle size and tidal flows, and consequently potential differences in plume dispersion patterns and concentrations, across the development area. The plume extents from the three modelled simulations are then transposed across the entire development area to produce a boundary containing the indicative worst case 'outer extent' of increases in suspended sediment concentration.

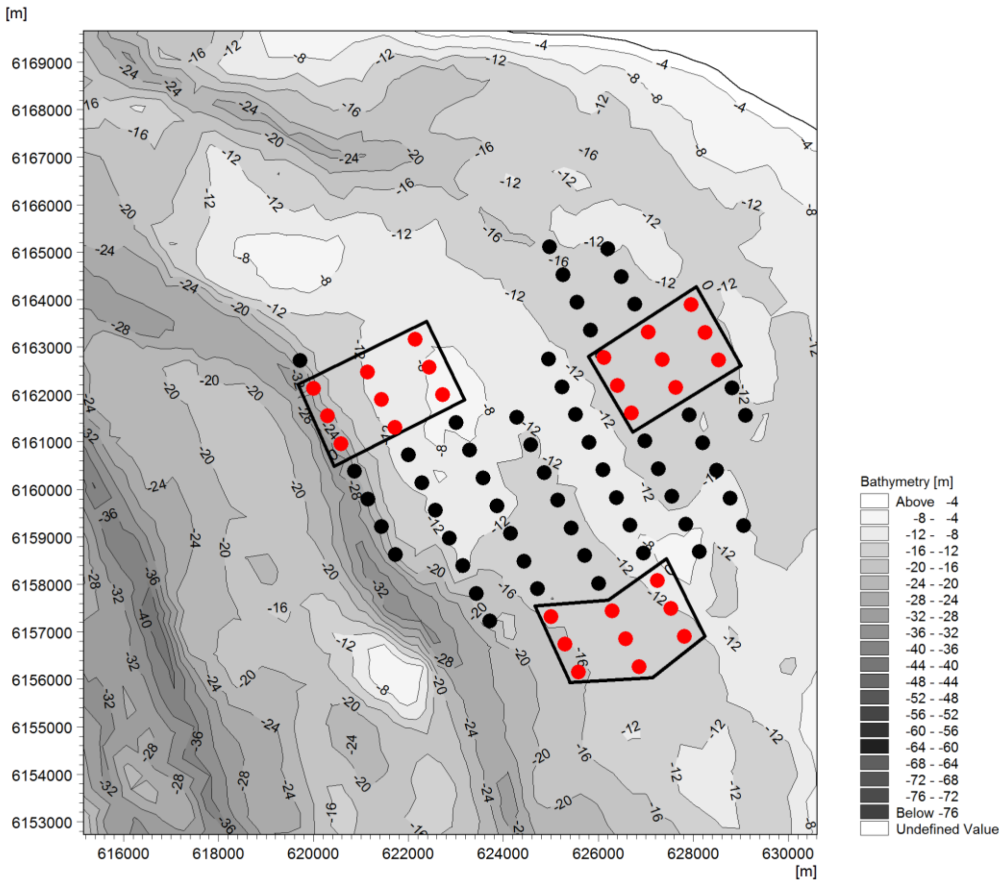

Figure 3.1. Location of foundations (in red) for worst case scenario construction.

The worst case scenario adopted here is a proportionate and practical approach, which is suitable to cover sediment dispersion from the entire site over the entire construction programme. This is because it is an intensive (i.e. very conservative) construction sequence and a less intense situation (i.e. longer term diffuse sediment dispersion) would be within those bounds. The construction of the entire site would mean that the location of the 'source' of sediment would move across the site as the installation progresses and from each source the dispersion patterns will take the sediment along a similar tidal stream, but to a different end destination. Hence, an interpretation

/ extrapolation of the results from the three sets of nine conical GBS foundations provide the intensive (i.e. worst case) basis for those assessments.

3.1.1 Seabed Preparation for Foundations

Seabed preparation is potentially required for GBS foundations in order to provide them with a stable surface on which to sit. An assumption is made that seabed preparation will be carried out using a dredger or an excavator placed on a barge or other floating vessel. The seabed preparation at each foundation is expected to take three days (based on Horns Rev 3; Energinet.dk, 2013) and will be continuous (i.e. 27 days for nine foundations). An assumption is made that three excavator vessels are operating simultaneously at the three sets of nine foundations. **After the three day installation it is assumed that scour protection is applied immediately to the foundation and no scour takes place**. As a worst case, each foundation will have 1,300m^3 of sediment excavated for seabed preparation over the three day period (based on Horns Rev 3; Energinet.dk, 2013 suggested 900-1,300m^3 per foundation). Of this 1,300m^3 a conservative estimate of 5% (65m^3) is released into the water column for dispersion, equating to a release rate at each foundation of 0.00025m^3/sec. The remainder (95%) is secured on barges for disposal (based on Horns Rev 3; Energinet.dk, 2013).

3.1.2 Jetting the Inter-array Cables

The worst case installation method for the inter-array cables is considered to be jetting. The volume of sediment affected during cable laying is 1.5m^3 per metre of jetting, assuming jetting to a worst case depth of 2m into the seabed, a triangular cross-section with a worst case top width of 1.5m (Figure 3.2). Using an excavation rate of 250m per hour (based on various estimates of jetting rates of between 150m and 450m per hour quoted by offshore developers), equates to a release rate of 0.1m^3/sec, which is 415 times higher than the sediment release rate of 0.00025m^3/sec for GBS foundation seabed preparation. Cables will be installed from north-northwest to south-southeast along each line of foundations proceeding from east to west (six cables per block of nine foundations). At a rate of 250m per hour, each cable would be completed in just over 2.6 hours because they have lengths of approximately 650m.

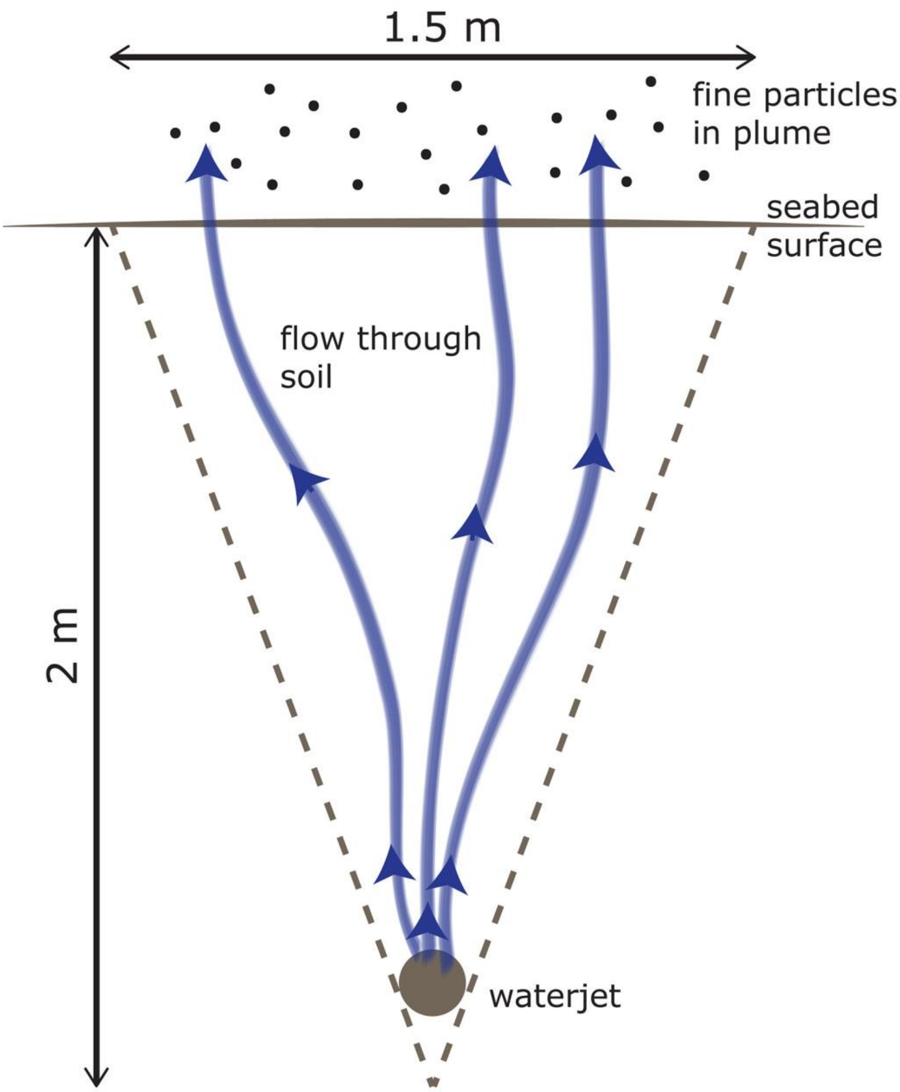

Figure 3.2. Process of jetting in cross-section.

3.1.3 Particle Size

Table 2.2 summarises particle size distributions for surface sediment samples recovered across Jammerland Bight. A conservative particle size distribution for sediment released due to seabed preparation is based on the maximum amount of fines (very fine sand and mud) in each of the samples. The particle size distributions in samples 14586, 14587 and 14589 were chosen to represent the sea bed sediment in the north-east, southern and northwest blocks, respectively.

3.2. Worst Case Construction Process for the Export Cable

The Jammerland Bight export cable corridor is approximately 4km long from its exit point at the development area to the landfall at Østrup. A variety of techniques could be used to excavate a trench for the export cable, but the worst case method is considered to be jetting.

3.2.1 Jetting the Export Cable

Installation of a single cable in a trench over a 2-day simulation period was modelled as the worst case scenario. Given an excavation rate of 250m/hour, the trench would be completed in about 16 hours. The volume of sediment released during cable laying is 1.5m^3 per metre of jetting equating to a release rate of 0.1m^3/sec (the same as for the inter-array cables, Figure 3.2).

3.2.2 Particle Size

Sample 14585 is the only one that is located on the export cable route (Figure 2.11) and was therefore chosen to represent the sea bed sediment along the entire route. It is assumed that this sediment is consistent to 2m sub-bottom.

4. TIDAL CURRENT MODEL SET-UP AND BASELINE CONDITIONS

The tidal current regime is defined as the behaviour of bulk water movements driven by the action of tides. In order to investigate tidal current flows across the western Baltic Sea and provide a baseline for prediction of changes due to Jammerland Bight, a hydrodynamic model was run for a 30-day simulation period.

MIKE21-HD and MIKE3-HD hydrodynamic models have been used to understand tidal current changes. MIKE21 is a widely used, state of the art integrated modelling package for application in coastal and port areas and was developed for simulation of non-steady water flow and transport of dissolved matter (DHI, 2014a). The hydrodynamic (HD) modules in both MIKE 21 and MIKE 3 solve the equations for the conservation of mass and momentum as well as for salinity and temperature in response to a variety of forcing functions.

The two-dimensional (2D) MIKE21-HD was used in the one layer mode, where current velocities predicted by the model are depth-averaged. The three-dimensional (3D) MIKE3-HD was used in the multiple vertical layer mode. The 3D model uses a vertical 'sigma-depth' and/or 'z-level' to calculate the 3D flow at different layers in the water column (Figure 4.1). The 'sigma depth" mode operates from the sea surface to 24m water depth, using 16 layers, with a vertical grid scale of about 0.9m near bed gradually increasing to 1.7m near surface (changes slightly due to tides). In the 'z-level' mode (from -24m below the sea surface), 30 layers are applied. The seabed in the development area is between -8m and -24m, so is entirely within the 'sigma depth'. The model results can be presented for each layer from the sea surface to the seabed.

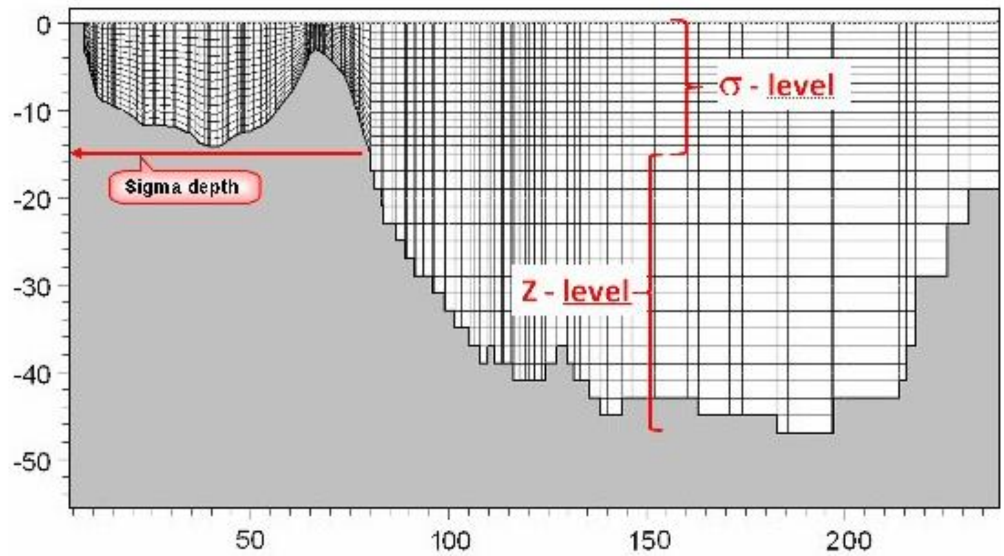

Figure 4.1. Schematic (not scaled to represent the actual model parameters) of sigma-depth and z-level in the 3D model.

The modelling was based on integration and downscaling from a large scale (regional model) to a small scale (local model) of tidal currents. The 2D MIKE21-HD was used for the regional model to simulate the large-scale circulation patterns of the coastal areas of the Danish Baltic Sea and North Sea. This regional model provided the boundary conditions as input to the more detailed 3D MIKE3-HD local model at and around the development area. It was applied to calculate the detailed tidal current patterns around the development area.

For each of the 2D regional and 3D local model, the following activities were completed:

1. Model calibration. The optimum model parameters are defined, i.e. the combination of parameter settings that give the most accurate model results when compared to measurements. The boundary conditions for the local 3D model are derived from the 2D regional model. The 3D model accounts for the spatial variations of salinity and temperature.
2. Model verification. The calibrated models are re-run with another period to check their implementation.
3. 3D model preparation and flow modelling. After the 2D model calibration and verification, the boundary conditions for input to the 3D model are produced. After 3D model calibration, the model production runs were performed to determine the changes to flow patterns (current velocities, current direction, salinity and temperature) caused by the proposed wind farm.

4.1. Model Bathymetry and Computational Mesh

Computational grids were created in order to model the tidal current flow patterns for the baseline condition (2D) and conditions with the worst case wind farm in place. The grids describe the bathymetry in the model with enough detail to produce sufficiently accurate model results within acceptable simulation times. The size of the computational grids varies over the model domain, and has been refined in and around the wind farm area in order to provide a detailed representation of the tidal currents locally.

4.1.1 Regional Model Bathymetry

The regional bathymetry was constructed using C-MAP and surveyed data along with coastline positions digitised from Google Earth. The model bathymetry shown in Figure 4.2 has been generated by combination of these data sets.

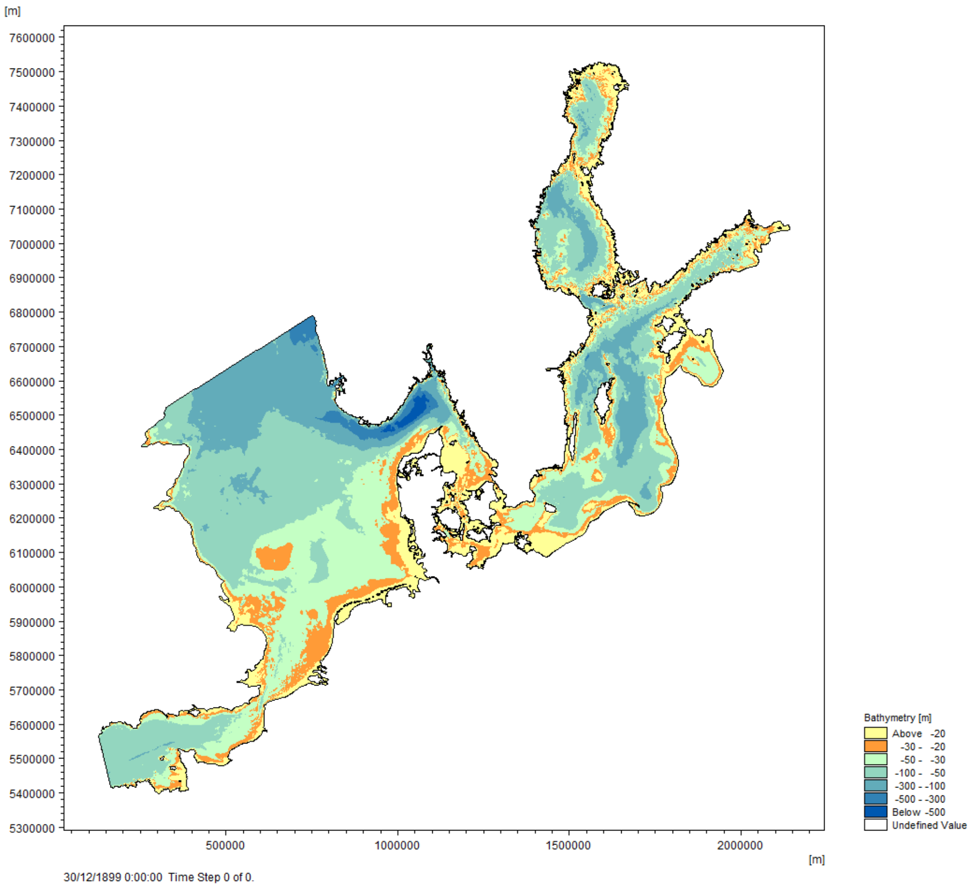

Figure 4.2. Bathymetry used in the regional 2D model domain.

4.1.2 Local Model

The model bathymetry and grid were locally updated with more detailed bathymetric survey data. The local model grid was developed for both the existing situation and the situation with the Jammerland Bight foundations in place (Figures 4.3 and 4.4). The required model resolution for the wind farm area is achieved by locally refining the mesh. The local mesh consists of 58,843 elements and 32,720 nodes and has different levels of resolution. The size of the computational cell varies over the model domain, and the model was refined in and around the wind farm in order to provide a detailed representation of the tidal currents. The local mesh has a fine resolution (about 300m) at the wind farm.

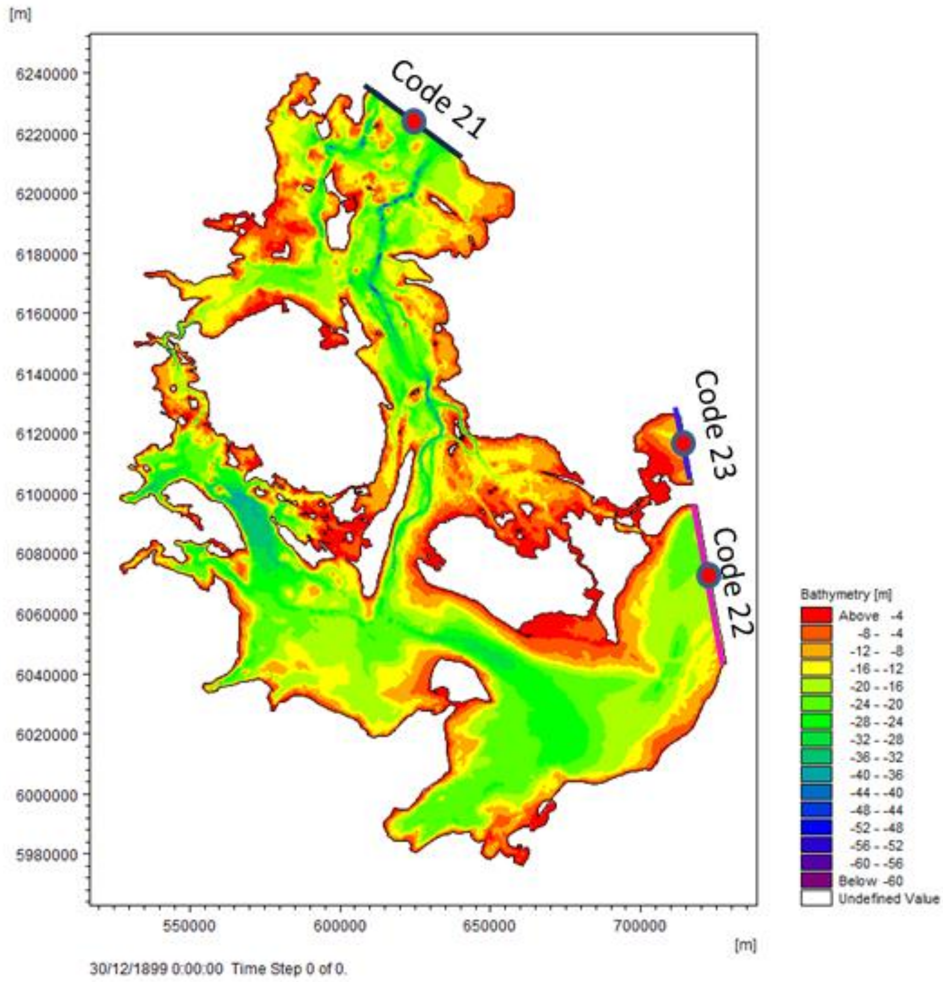

Figure 4.3. Bathymetry used in the local 3D model domain and location of the open boundaries.

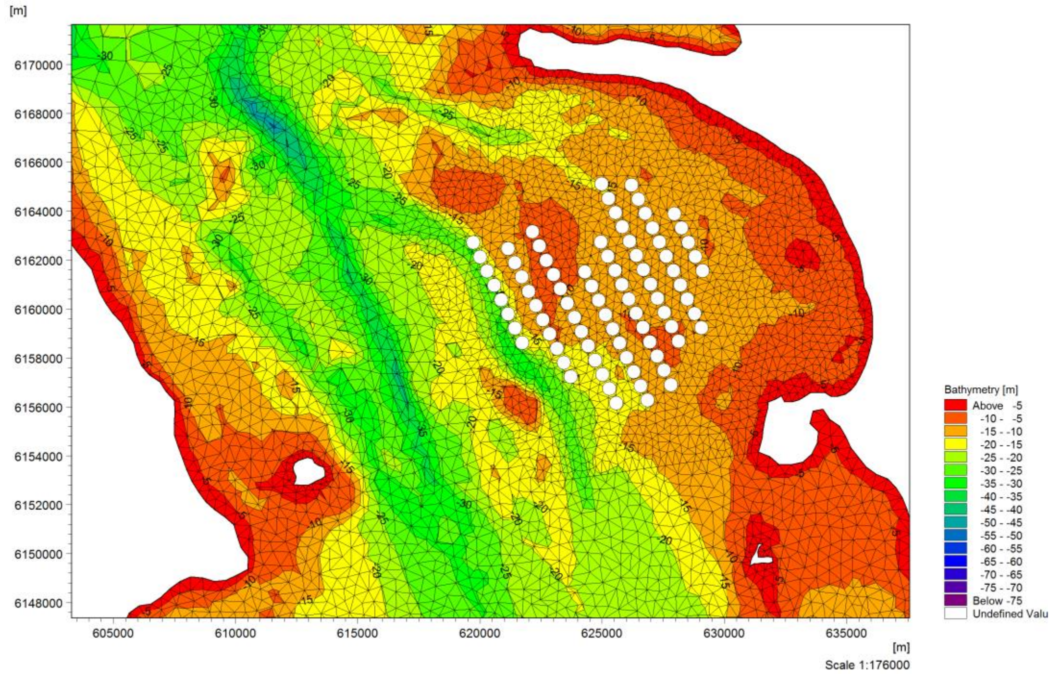

Figure 4.4. Bathymetry and computational mesh in and around Jammerland Bight.

4.2. Boundary Conditions

The open boundaries of the regional model are set to water level boundaries, varying in time and space along the boundaries. These data were extracted from the global tide model, which represents the major diurnal (K1, O1, P1 and Q1) and semidiurnal tidal constituents (M2, S2, N2 and K2) with a spatial resolution of 0.25º x 0.25º based on OPEX/POSEIDON altimetry data.

The three offshore open boundaries (Figure 4.3) are set to water level boundaries varying in time and along the boundary. The water level boundaries are extracted from the regional model for a period of 40 days from 20th November 2013 to 30th December 2013. The time series of water levels for December 2013 at the open boundaries are shown in Figure 4.5. The tidal ranges are typically less than 0.5m for all boundaries. The water fluctuations at the northern boundary (Code 21) show a wind set-up during the extreme storm event on 6-7th December 2013 while the water fluctuations at the two eastern boundaries (Codes 22 and 23) show a wind set-down. Figure 4.5 also shows that the definition of the spring neap cycle is unclear because the boundaries are not exposed to the open sea. The boundary conditions for the local 3D model are derived from the 2D regional model.

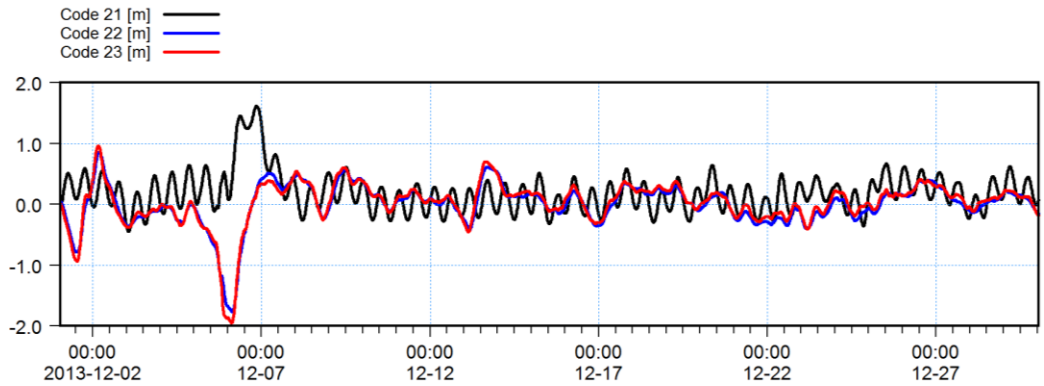

Figure 4.5. Time series of water level boundary conditions for the local model. Position of the boundaries is shown on Figure 4.3.

4.3. Model Calibration

In order to accurately simulate tidal currents, the regional and local models were calibrated. Calibration is the process of defining the optimum model parameters, so the model results are as close as possible to the measured data (tidal current velocities and water levels).

For the 2D regional model, the calibration was based on measured water levels from 10 stations around the Kattegat (Figure 2.3). The model was calibrated using a period of one month, from 1st to 31th December 2013. This time period had the strongest wind condition of that year and covers the extreme surge event on 6-7th December 2013 (Cyclone Xaver). It is expected that if the model can capture the worst case condition then it can also predict other periods with milder wind conditions.

Wind variations are an important aspect of the physical processes in the Great Belt. Surface wind has significant variation over a large area and can have a large impact on the surface elevation and current conditions. Therefore, the calibration process primarily included the adjustment of the wind friction (using the results from the DHI SKA model) until good agreement was obtained between the simulated and measured current velocity and water levels. The spatial variation of the air pressure is also important and is included in both the 2D and 3D models.

For the 3D local model, the current meter at Østerrenden is close to the development area and the recorded data was used over the calibration period. The calibration period was ten days from 1st to 10th December, which includes the extreme storm event. Modelled tidal current data from Point 6 (located in the local model domain) was also used. The calibration with the modelled tidal current data (DMI) contains the comparisons of the vertical current profile (velocities and directions), salinity and temperature, for the surface layer, middle layer and bottom layer. These two locations are shown in Figure 4.6.

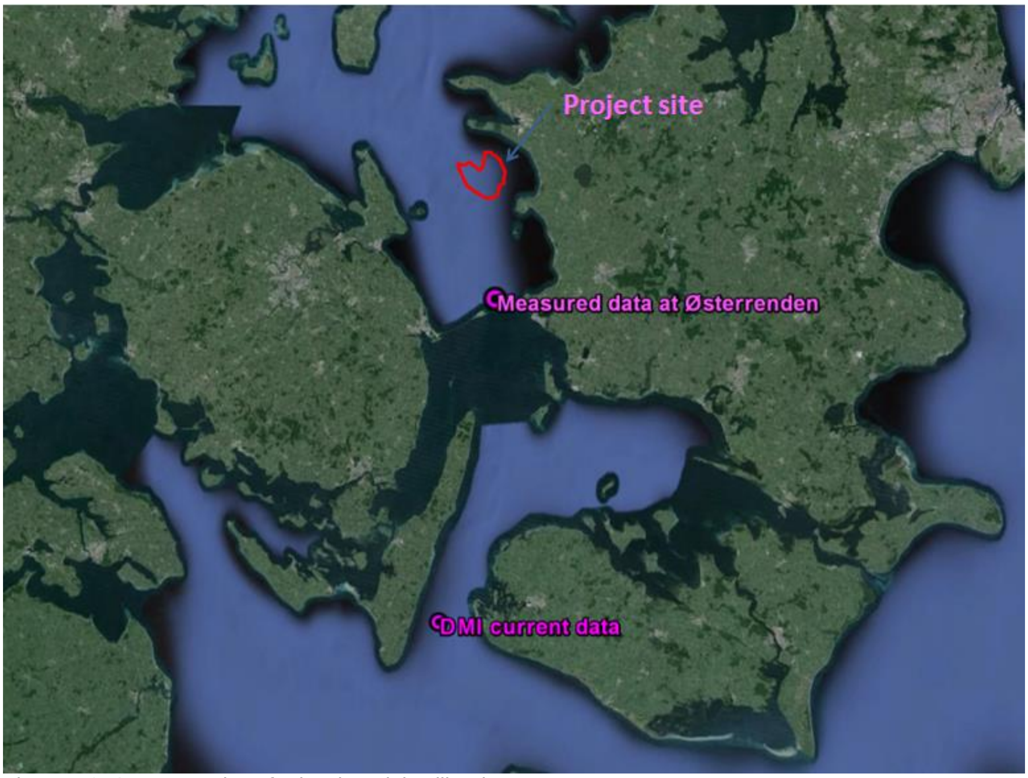

Figure 4.6. Current stations for local model calibration.

The results of the model calibration are presented in Appendix A.

4.4. Modelled Baseline Tidal Current Velocities

A model production run was completed to determine the baseline (existing) tidal current velocities and current direction in the vicinity of Jammerland Bight. Currents were simulated for a one month period from 1st to 30th December 2013. This covers the extreme surge event that occurred on 6-7th December 2013 caused by cyclone Xaver. For the assessment of the effect of the wind farm on the hydraulic condition, the flow field at 10:00am on 6th December 2013 was considered, corresponding to the peak current condition during the extreme event.

Figures 4.7 to 4.9 present the predicted peak current velocities in the bottom, middle and surface layers in the vicinity of the wind farm. Within the development area, the predicted bottom currents range from 0.3m/s to 0.6m/s (8m-24m below mean sea level). The current velocities are higher along the west side of the proposed wind farm, which is closer to the main flow of the Great Belt. In the middle layer, the current velocities are slightly increased. Near the sea surface of the proposed wind farm area, the predicted current velocities further increase, ranging from 0.7m/s to 1.2m/s.

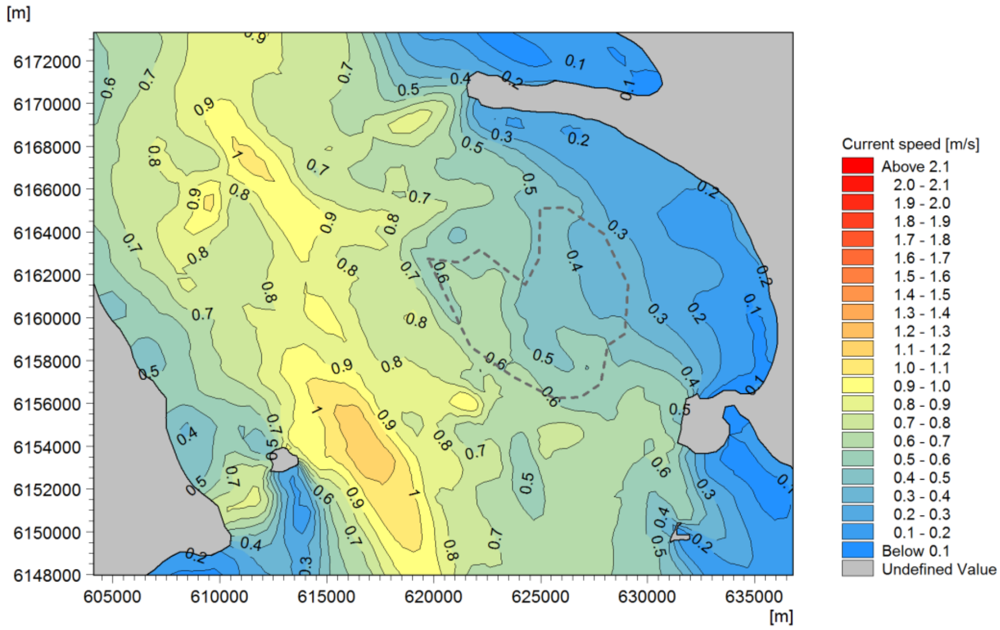

Figure 4.7. Simulated current velocities extracted at 10.00am on 6th December 2013 in the bottom layer.

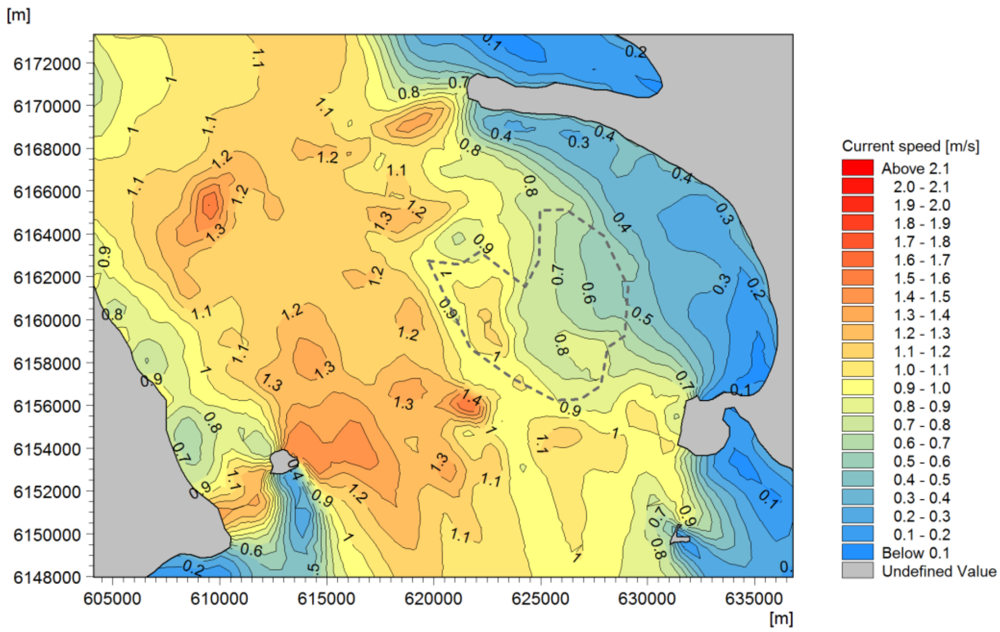

Figure 4.8. Simulated current velocities extracted at 10.00am on 6th December 2013 in the middle layer.

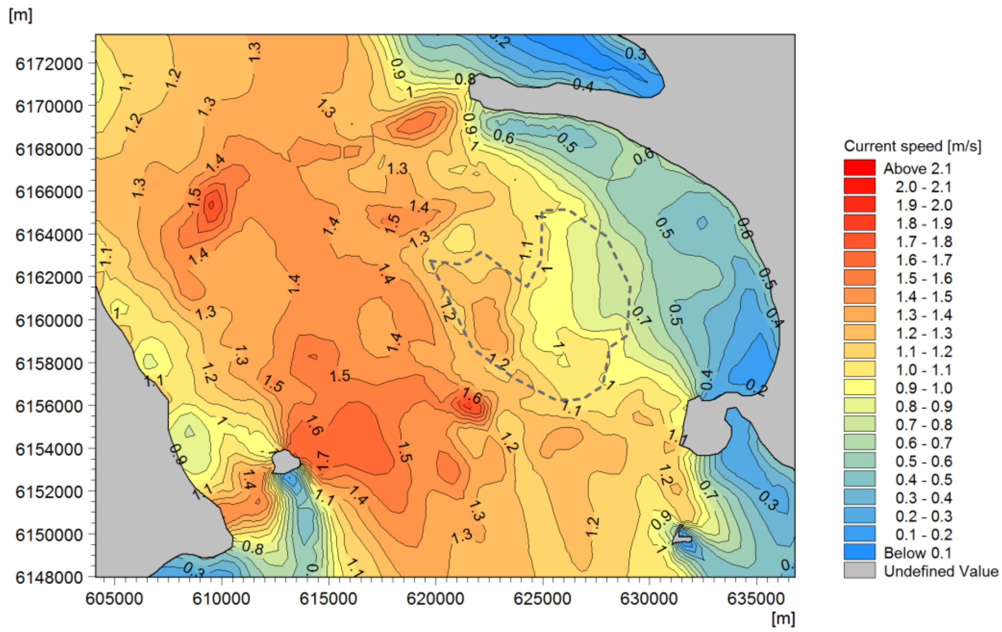

Figure 4.9. Simulated current velocities extracted at 10.00am on 6th December 2013 in the surface layer.

4.5. Sediment Plume Dispersion Model

Over the construction period, there is potential that the seabed will be disturbed. Installation of foundations and cables will generate additional suspended sediment into the water column, which may result in the formation of sediment plumes. The mobilised sediment may then be transported away from the disturbance by tidal currents. The magnitude of the plume will be a function of seabed type, the installation method and the tidal current conditions in which dispersion takes place.

Mobilisation of sediment on the seabed occurs when the tidal current forces exert a shear stress that exceeds a threshold relevant to the sediment type. When shear stress drops below this threshold, the sediment begins to fall out of suspension and is re-deposited on the seabed. If the shear stress is then increased above the threshold again, the sediment will be re-suspended. It is, therefore, possible for sediment to be continually re-deposited and re-suspended, as tidal conditions change. Typically, finer sediments are suspended at lower shear stresses compared to coarser sediments, and will remain in the water column for longer periods of time. Coarser sediments are more likely to be transported as bedloads.

The simulation of the release and spreading of fine sediments as a result of foundation and cable installation activities have been modelled using the 3D model MIKE3-FM Mud Transport (MT) (DHI, 2014b). MIKE3-FM MT is integrated with MIKE3-FM HD, which has been used to predict tidal current velocity changes, and takes into account:

- the actual release of sediments as a function of time, location and sediment characteristics;

- advection and dispersion of the suspended sediment in the water column as a function of the 3D flow field predicted by MIKE3-FM HD; and
- settling and deposition of the dispersed sediment.

4.5.1 Model Parameterization

The available sediment from seabed preparation and cable jetting has been released into the bottom layer. Table 4.1 presents the size fractions of the seabed sediment (location of samples is shown in Figure 2.11). Sample 14585 was chosen to represent bed sediment along the export cable route, in which 32.75% of sediment is silt and clay and 60.23% is very fine sand. Sample 14589 and 14586 were chosen to represent bed sediment in the northwest and northeast parts of the development area, respectively. Sample 14589, contains 0.33% silt and clay, 0.46% very fine sand and 25.57% fine sand, and sample 14586 contains 72.42% silt and clay, 15.63% very fine sand and 8.71% fine sand. The southern part of the development area has been modelled using sample 14587, which contains 0.82% silt and clay, 1.38% very fine sand and 12.80% fine sand. The release of sediment results in dispersion that has been estimated as suspended sediment concentration in excess of zero sediment concentration.

Table 4.1. Sediment size and fraction.

Sediment Type (size in mm)	Percentage in Sample					
	14584	14585	14586	14587	14588	14589
Very coarse sand & gravel (>1)	0.23	0.21	1.90	39.33	1.49	4.85
Coarse sand (0.5-1)	0.14	0.12	0.44	16.08	0.31	4.91
Medium sand (0.25-0.5)	0.24	0.44	0.90	29.59	0.12	63.88
Fine sand (0.125-0.25)	37.58	6.25	8.71	12.80	1.87	25.57
Very fine sand (0.063-0.125)	47.48	60.23	15.63	1.38	18.17	0.46
Silt & clay (<0.063)	14.33	32.75	72.42	0.82	78.04	0.33

The sediment fraction simulated by the model is defined by its settling velocity and its critical shear stress. Table 4.2 presents the adopted sediment settling velocity and critical shear stress. A sediment density of 1,590kg/m^3 has been used to represent the undisturbed seabed sediments, assuming a porosity of 0.4 and a density of dry sediment of 2,650kg/m^3.

Table 4.2. Sediment settling velocity and critical bed shear stress.

Sediment Type	Fall velocity (m/s)	Critical bed-shear stress (N/m^2)
Gravels	0.1142	0.4806
Coarse sands	0.0663	0.2616
Medium sands	0.02874	0.1895
Fine sands	0.00868	0.1530
Very fine sands	0.002279	0.1201
Silts and clays	0.000519	0.0831

The modelling of sediment dispersion for foundation seabed preparation and inter-array cable jetting was carried out over a 30-day simulation period using the baseline 30-day hydrodynamic simulation. The dispersion from the shorter installation of the export cable was modelled over a 2-day period. The sediment along the inter-array and export cables was released continuously for dispersion as the excavation progresses.

5. POTENTIAL PRESSURES DURING CONSTRUCTION

The construction phase of Jammerland Bight has the potential to affect hydrography and sediment spill both locally and further afield. Offshore construction activities include installation of the foundations and laying of inter-array and export cables, all of which may affect the tidal current regime and sediment transport processes.

The results of the sediment plume dispersion modelling are presented as a series of maps showing maximum suspended sediment concentration in the bottom, middle and surface layers of the water column and sediment deposition on the seabed from the plume, using the following statistical measures over the simulation period:

- the maximum values of suspended sediment concentration in each layer;
- the time over which suspended sediment concentration exceeds 10mg/l; and
- the maximum thicknesses of deposited sediment.

The threshold of 10mg/l was adopted because many marine organisms are sensitive to concentrations around 10mg/l. This is an indicative value used by many marine biologists for pelagic fish (Orbicon, 2014).

5.1. Increase in Suspended Sediment Concentrations and Deposition as a Result of Foundation Installation

Figure 5.1 shows the maximum suspended sediment concentration in the bottom layer, predicted by the model at any time over the 30-day simulation period for foundation seabed preparation only. Predicted maximum suspended sediment concentrations are hardly increased above baseline levels at each of the foundations. The same result applies to both the middle and surface layers. Figure 5.2 shows that the predicted suspended sediment concentrations never exceed 10mg/l for seabed preparation only.

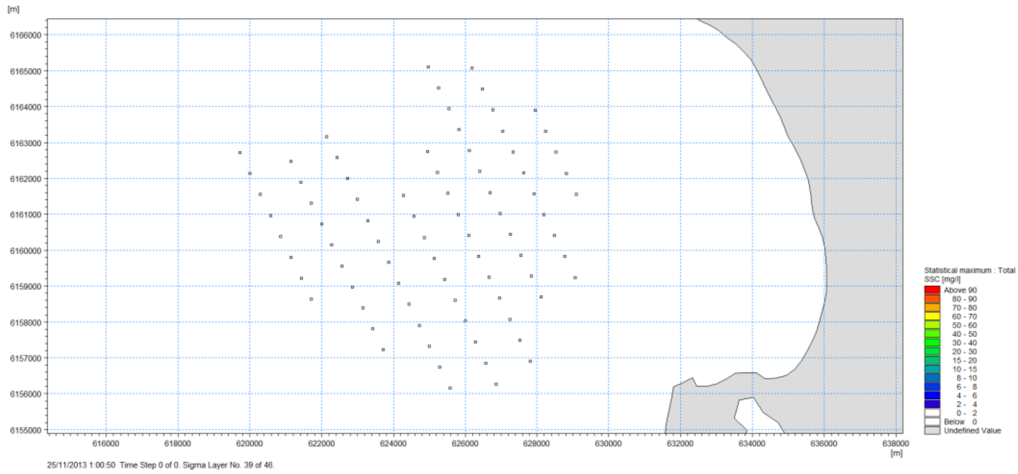

Figure 5.1. Maximum suspended sediment concentration (mg/l) in the bottom layer predicted over the simulation period for the construction phase for the GBS foundations only.

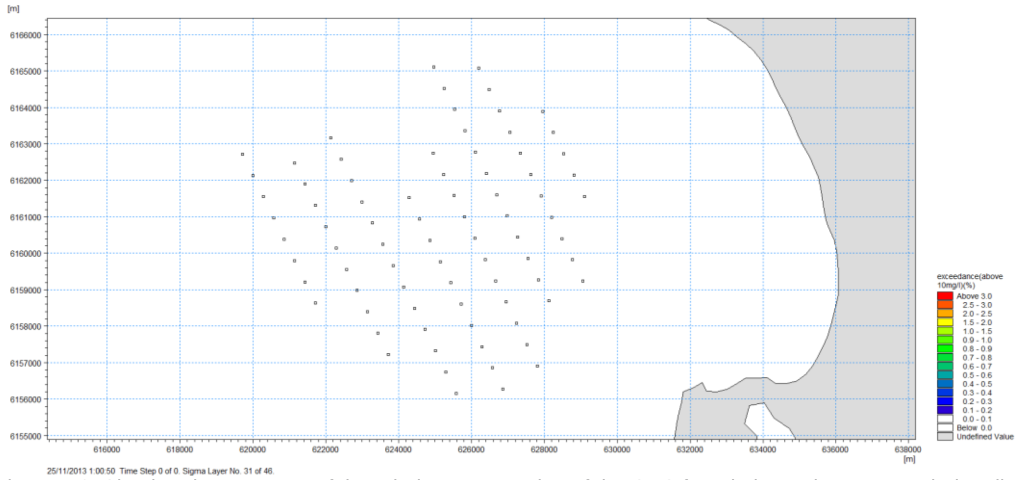

Figure 5.2. Simulated percentage of time during construction of the GBS foundations when suspended sediment concentrations in the bottom layer exceed 10mg/l.

Figure 5.3 shows the maximum change in deposition predicted at any time over the 30-day simulation period for seabed preparation only. The largest predicted maximum change is less than 4mm in a very small patch close to a single foundation in the southwest corner of the development area. At all the other foundations modelled, the maximum change is predicted to be less than 2mm.

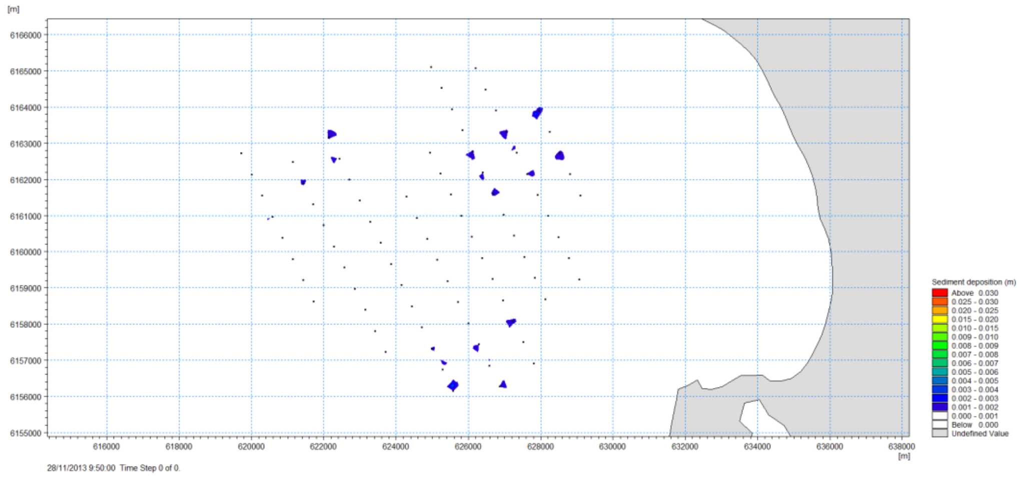

Figure 5.3. Maximum deposition (mm) from the plume for the construction phase for GBS foundations only.

The model predictions using the three blocks of foundations show that increases in suspended sediment concentrations are limited to areas adjacent to the foundations. To expand this analysis to include installation of all foundations, the results from the three blocks can be transposed across the entire development area to create a boundary containing the indicative worst case 'outer extent' of the sediment plume. Consequently, the overall sediment plume would be contained within the development area. The extent of plumes from each foundation would be at the same scale or less than those modelled, thus of low magnitude. Hence, the Magnitude of Pressure of additional suspended sediment in the water column caused by construction of foundations is considered to be low.

5.2. Increase in Suspended Sediment Concentrations and Deposition as a Result of Inter-array Cable Installation

Figures 5.4 to 5.6 show the maximum suspended sediment concentration in the bottom, middle and surface layers predicted by the model at any time over the 30-day simulation period for inter-array cable installation only. The figures show that sediment plumes are predicted to occur across the northeast block of nine foundations only. This is because the volume of silt and clay input to the model is high for the northeast block (72%, sample 14586) compared to the northwest and south blocks (less than 1%, samples 14589 and 14587).

Across the northeast block, maximum suspended sediment concentrations of 60mg/l to over 90mg/l were predicted in the bottom layer along the line of each inter-array cable (Figure 5.4). However, these highest values are very restricted in geographical extent (patches up to about 300m wide and 500m long) and the majority of the plumes have maximum suspended sediment concentrations of less than 50mg/l. The predicted maximum suspended sediment concentrations reduce to zero within about 350m of the cable transects in all directions. At shallower depths, the suspended sediment concentrations reduce to a general maximum of about 10mg/l in the middle layer (in some places there is no effect) (Figure 5.5). In the surface layer, maximum suspended sediment concentrations reduce further, to effectively zero, with an isolated patch up to 6mg/l (Figure 5.6).

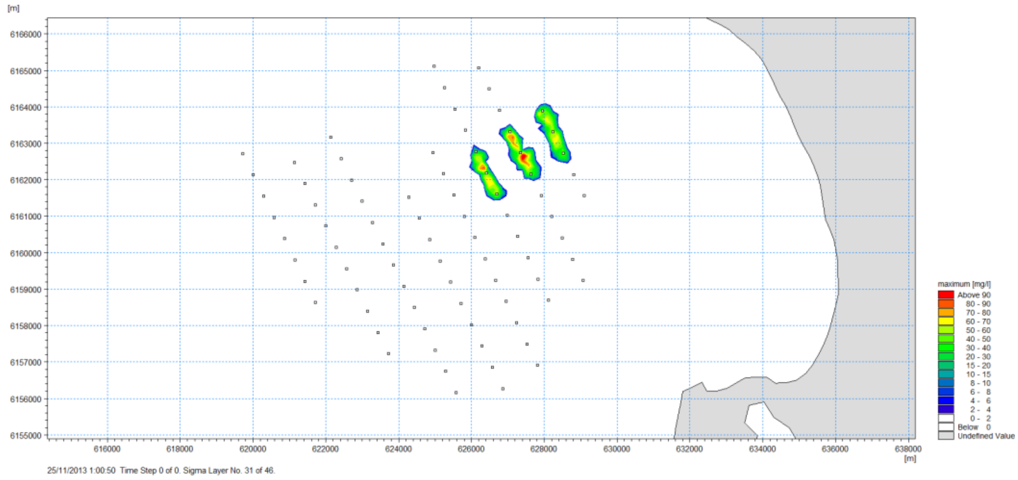

Figure 5.4. Maximum suspended sediment concentration (mg/l) in the bottom layer predicted over the simulation period for inter-array cable installation.

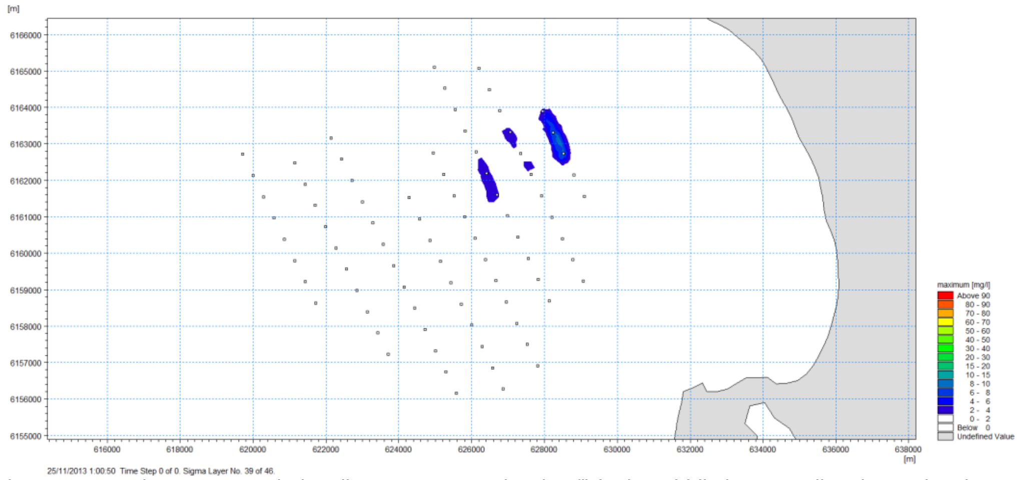

Figure 5.5. Maximum suspended sediment concentration (mg/l) in the middle layer predicted over the simulation period for inter-array cable installation.

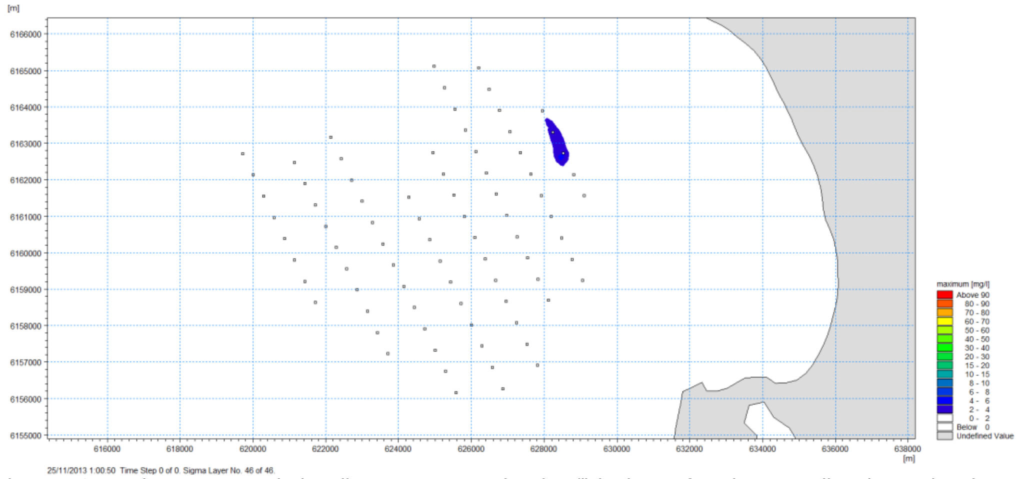

Figure 5.6. Maximum suspended sediment concentration (mg/l) in the surface layer predicted over the simulation period for inter-array cable installation.

Figures 5.7 and 5.8 present the percentage of time of the entire simulation period (30 days) when the predicted suspended sediment concentrations in the bottom and middle layers exceed 10mg/l for cable jetting. For cable jetting, 10mg/l is predicted to be exceeded less than 1% of the 30-day simulation period. In the surface layer, the predicted suspended sediment concentrations never exceed 10mg/l.

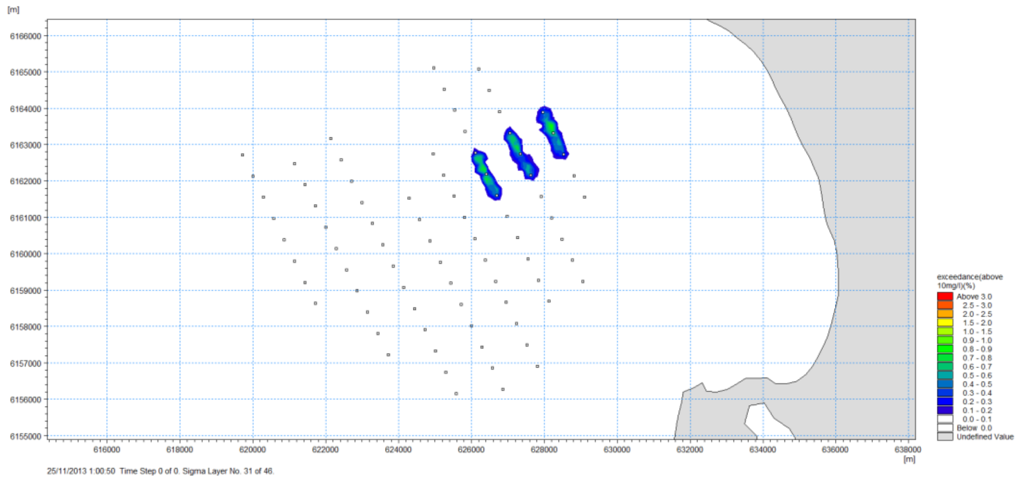

Figure 5.7. Simulated percentage of time during inter-array cable installation when suspended sediment concentrations in the bottom layer exceed 10mg/l.

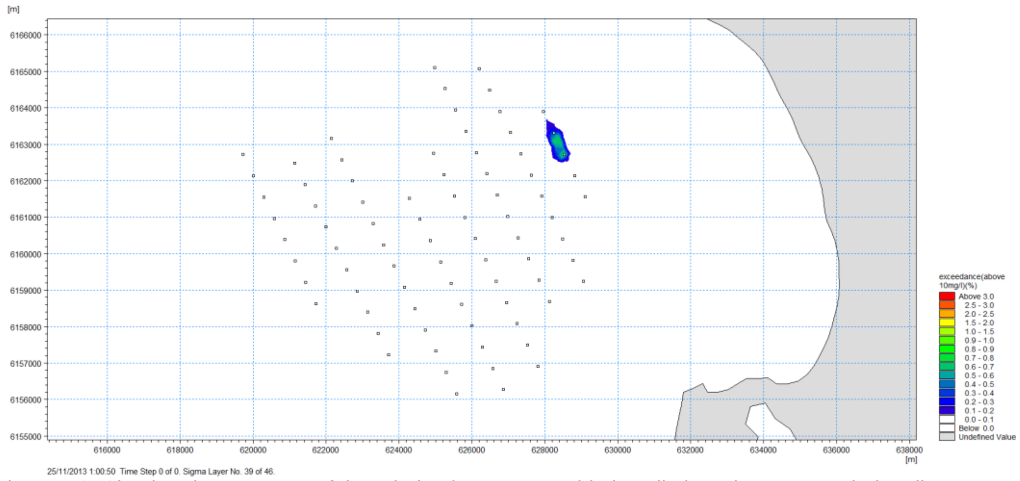

Figure 5.8. Simulated percentage of time during inter-array cable installation when suspended sediment concentrations in the middle layer exceed 10mg/l.

Figure 5.9 shows the maximum change in deposition predicted at any time over the 30-day simulation period for inter-array cable installation. The largest predicted maximum change for cable installation is approximately 20mm along the line of the cable. The predicted deposition decreases with distance from the cable, reducing to baseline values approximately 250m either side of the route.

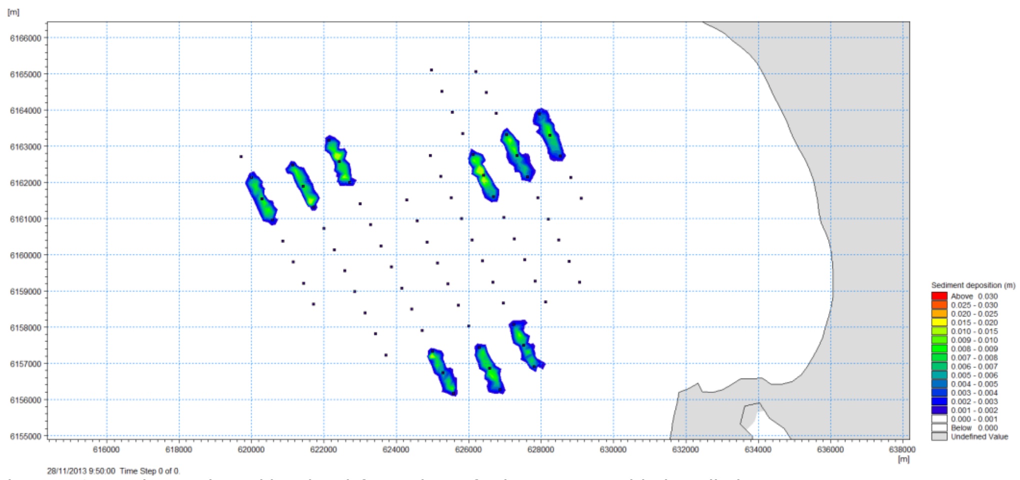

Figure 5.9. Maximum deposition (mm) from plume for inter-array cable installation.

If the individual deposition areas are transposed across the entire development area shows that deposition would be contained within the development area. The magnitude of deposition from each foundation would be at the same scale or less than those modelled. Given the dynamic and generally sandy nature of the substrate at Jammerland Bight, deposition of 20mm of sediment is likely to be very small compared to the natural variation of bed level changes across the area. Hence, the Magnitude of Pressure of additional deposition of sediment on the seabed caused by installation of inter-array cables (and foundations) is considered to be low.

5.3. Increase in Suspended Sediment Concentrations and Deposition as a Result of Export Cable Installation

Figures 5.10 to 5.12 show the maximum suspended sediment concentration predicted by the model at any time over the 2-day simulation period for jetting the export cable, for the bottom, middle and surface layers.

The worst effect is predicted in the bottom layer (Figure 5.10). This is to be expected, given the release point is at the sea bed. Predicted maximum suspended sediment concentrations in the bottom layer generally increase from the edge of the development area (less than 10mg/l) to higher concentrations of over 90mg/l towards the coast. This is related to gradually shallowing water and associated higher energies as excavation progresses from offshore towards the coast. Suspended sediment concentrations decrease with distance away from the cable, reducing to zero up to 300m west or east of the cable. At shallower depths in the water column, the suspended sediment concentrations reduce to a maximum near the coast of about 40mg/l in the middle layer (Figure 5.11). Concentrations reduce to effectively zero along the seaward half of the cable route. In the surface layer, suspended sediment concentrations reduce further, to less than 30mg/l locally at the coast (up to 1.5km offshore from the coast, Figure 5.12).

Given that the naturally induced suspended sediment concentrations can be several hundred mg/l during storm conditions indicates that concentrations due to jetting are within the scale of natural processes. Hence, the Magnitude of Pressure of additional suspended sediment in the water column caused by installation of export cable is considered to be low.

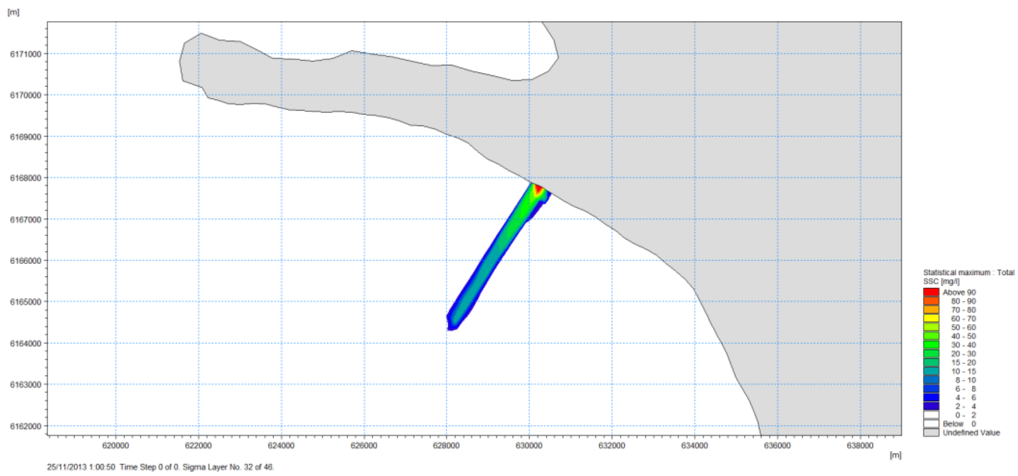

Figure 5.10. Maximum suspended sediment concentration (mg/l) in the bottom layer predicted over the simulation period for the construction phase of the export cable corridor.

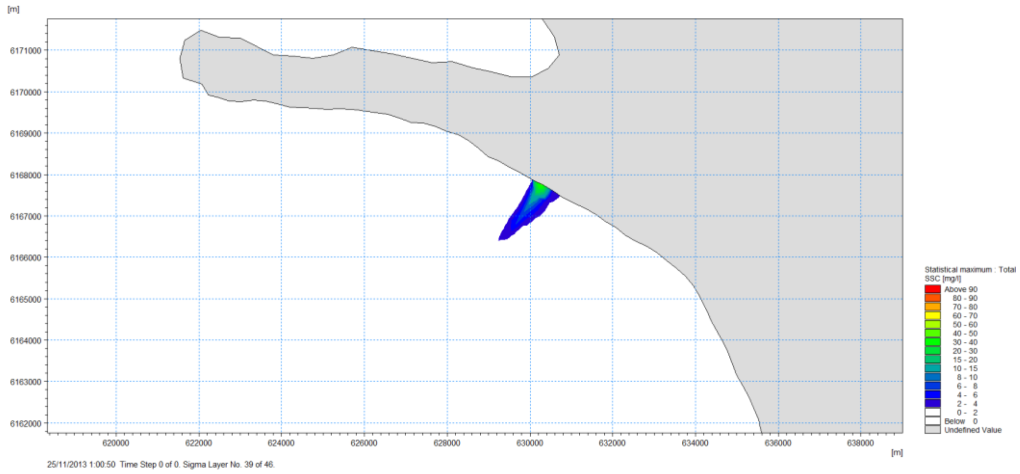

Figure 5.11. Maximum suspended sediment concentration (mg/l) in the middle predicted over the simulation period for the construction phase of the export cable corridor.

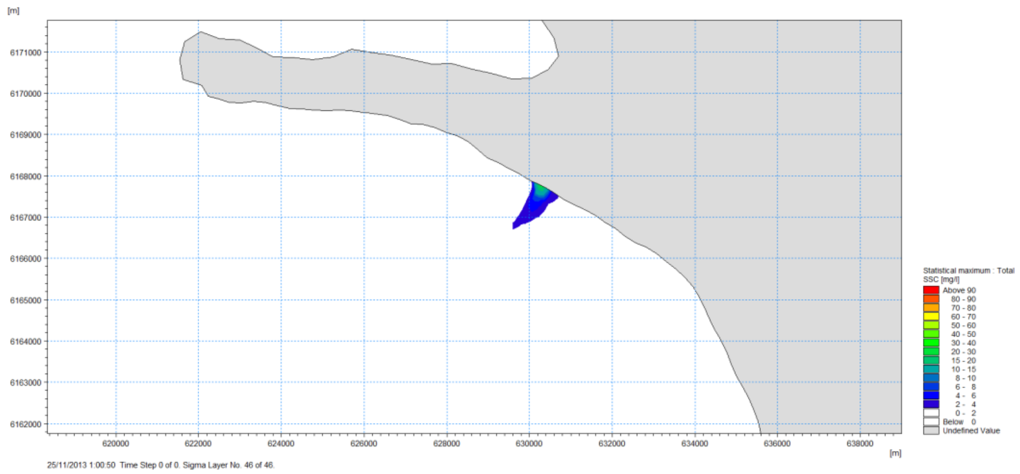

Figure 5.12. Maximum suspended sediment concentration (mg/l) in the surface layer predicted over the simulation period for the construction phase of the export cable corridor.

Figures 5.13 to 5.15 present the percentage of time of the entire simulation period (2 days) when the predicted suspended sediment concentrations exceed 10mg/l in the bottom, middle and surface layers, respectively. The maps show that 10mg/l is predicted to be exceeded less than 1% of the 2-day simulation period along the cable in the bottom layer, reducing to 0% a short distance (less than 250m) to the west and east. In the middle and surface layers, the suspended sediment concentrations exceed 10mg/l less than 2% and 1.5% of the simulation period.

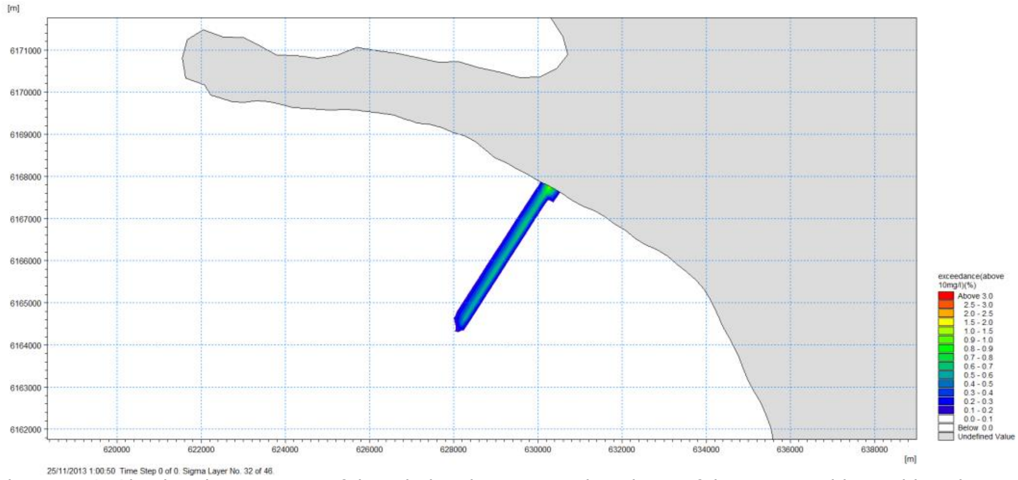

Figure 5.13. Simulated percentage of time during the construction phase of the export cable corridor when suspended sediment concentrations in the bottom layer exceed 10mg/l.

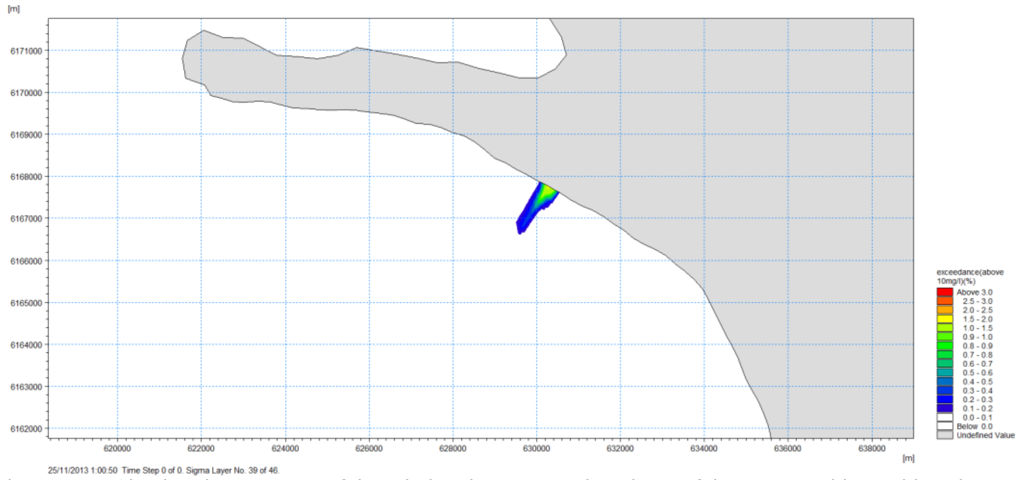

Figure 5.14. Simulated percentage of time during the construction phase of the export cable corridor when suspended sediment concentrations in the middle layer exceed 10mg/l.

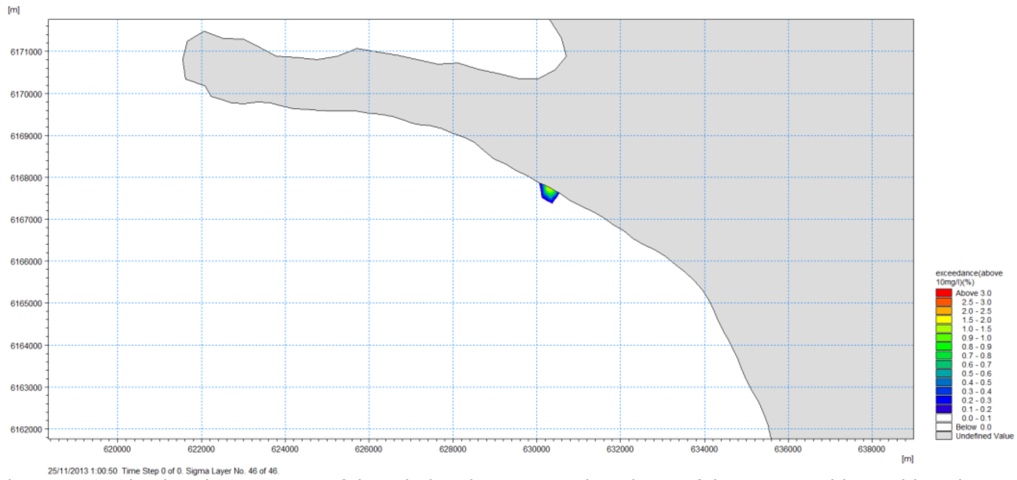

Figure 5.13. Simulated percentage of time during the construction phase of the export cable corridor when suspended sediment concentrations in the surface layer exceed 10mg/l.

Figure 5.16 shows the maximum change in deposition predicted at any time over the 2-day simulation period. The largest predicted change is less than 9mm local to the route of the cable. Predicted deposition from the plume reduces rapidly away from the cable corridor extending for no more than 200m to the west or east. Given the dynamic nature of the substrate along the export cable route, deposition of these magnitudes is within the natural variation of bed level changes. Hence, the Magnitude of Pressure of additional deposition of sediment on the seabed caused by installation of the export cable is considered to be low.

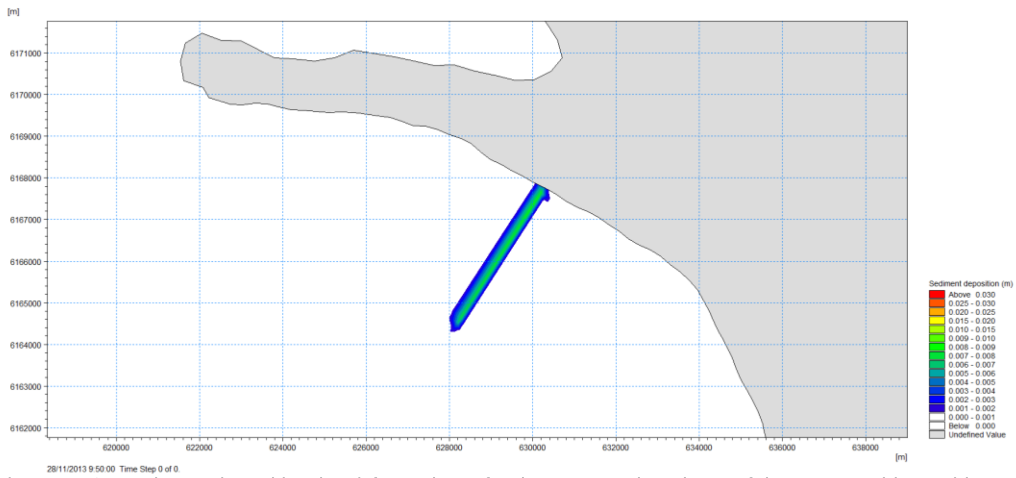

Figure 5.16. Maximum deposition (mm) from plume for the construction phase of the export cable corridor.

5.4. Pressures on Natura 2000 Sites of Construction Activities

Due to the limited, local and temporary magnitude of change of hydrography and sediment transport caused by construction of the wind farm and export cable, the Magnitude of Pressure is considered to be low.

6. POTENTIAL PRESSURES DURING OPERATION

The operational phase of the proposed Jammerland Bight offshore wind farm equates, at a minimum, to the duration of the lease (nominally 25 years). During this time, the hydrography and sediment spill effects of the development are likely to be evident through persistent and direct changes, resulting from tidal current interactions with the foundation structures. There are anticipated to be no hydrography and sediment spill effects during the operation of the inter-array cables or export cables, where they are buried beneath the seabed.

A wind farm comprising 80 3MW turbine foundations is proposed (see Section 1.3). Across the Jammerland Bight development area, the bathymetry varies from -8m to -24m mean sea level. Hence, the geometry of the foundations that have been modelled has been scaled in size to be appropriate for these depths. Foundation designs for 10m and 20m mean sea level water depth have been considered (Figure 6.1). The worst case foundation layout used in the simulation is shown in Figure 6.2 and comprises 3MW foundations across the entire development area. The 10m geometry foundations are used across the majority of the development area with 20m geometry foundations along the western edge, where the water is deeper.

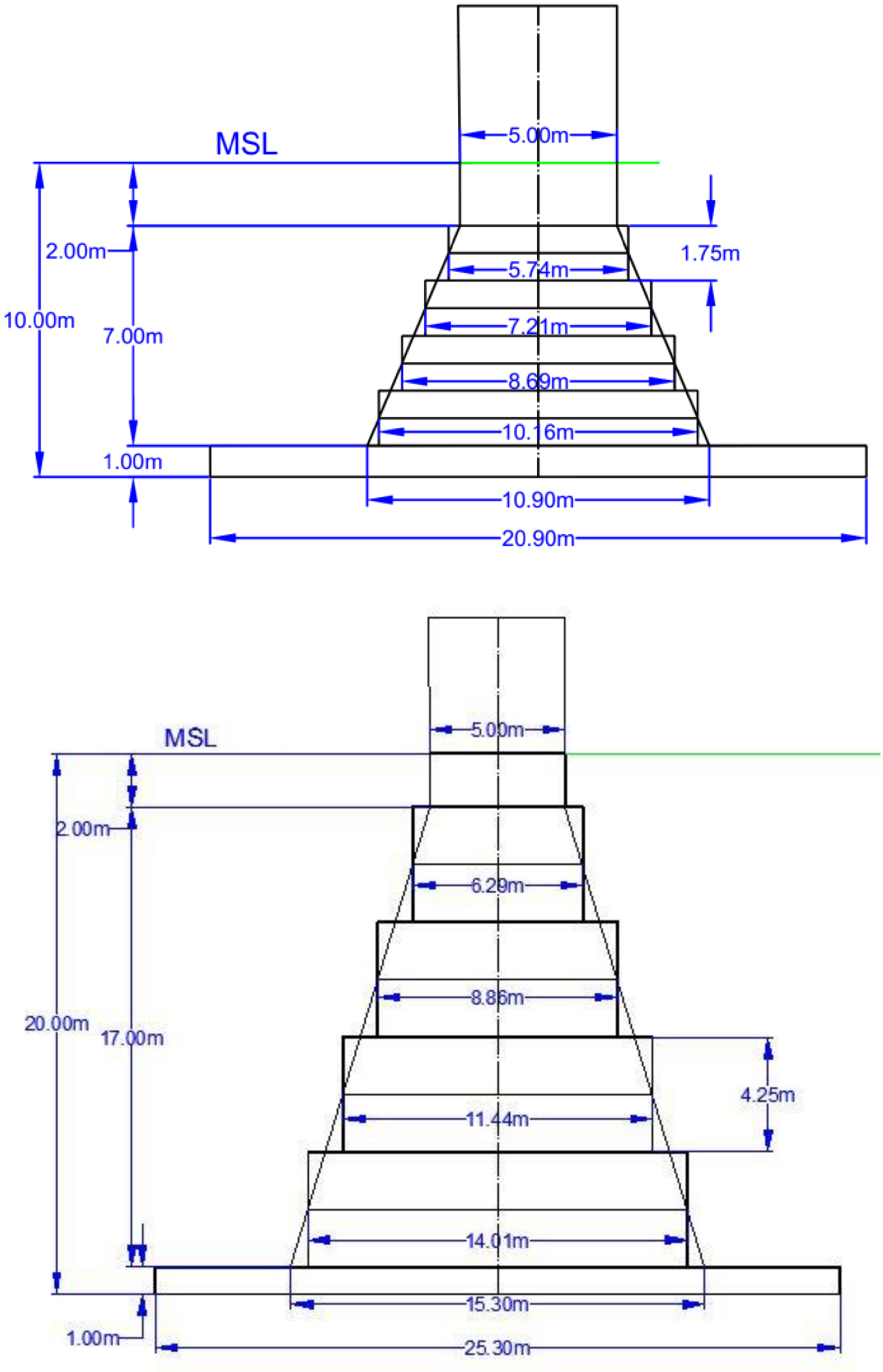

Figure 6.1. Geometries of the 3MW foundation for water depths of 10m (top) and 20m (bottom).

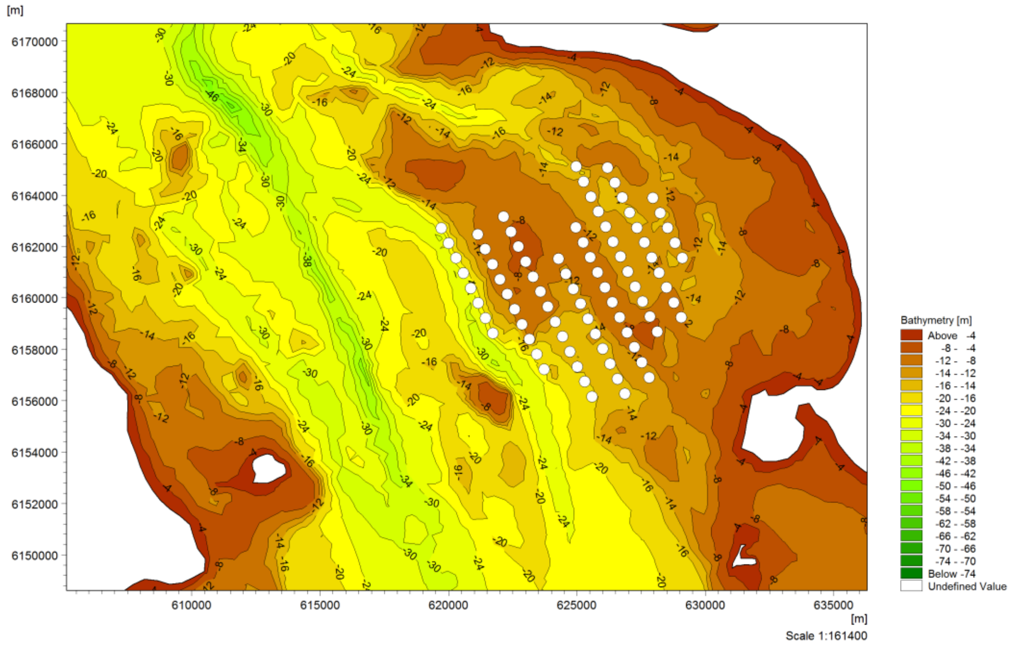

Figure 6.2. Layout of the 3MW foundations that was modelled.

6.1. Effect of Foundation Structures on Tidal Current Velocities

The effects on tidal current velocities of the foundation layout have been examined as changes at three depths relative to the baseline. The results of the hydrodynamic modelling are presented as a series of maps showing the maximum current velocity in the bottom, middle and surface layers relative to the baseline at 10am on 6th December 2013. Figures 6.3 to 6.5 describe the effect of the foundation layout on tidal current velocities showing the current velocities with the wind farm in place, the change in velocities and the percentage change in velocity relative to the baseline.

Due to the presence of the proposed foundations, the current velocities through the wind farm are reduced slightly. The maximum reduction is 0.001-0.006m/s over the entire water column. Current velocities increase slightly to the west and east of the wind farm due to constriction of the flow in Great Belt. There are almost no effects at the coast. The changes to the current velocities are limited to within the layout and to a maximum of 6km outside the layout boundary. This means the operation of the proposed wind farm is predicted not to affect the main flow through Great Belt. The effects are slightly greater in the surface and middle layers than the bottom layer. The presence of the foundations leads to a current variation of less than 1%.

The maximum difference in current velocity is less than 0.006m/s, demonstrating an overall inconsequential effect on tidal current patterns across Jammerland Bight and regionally. Hence, the Magnitude of Pressure of changes to tidal currents caused by operation of Jammerland Bight is considered to be low.

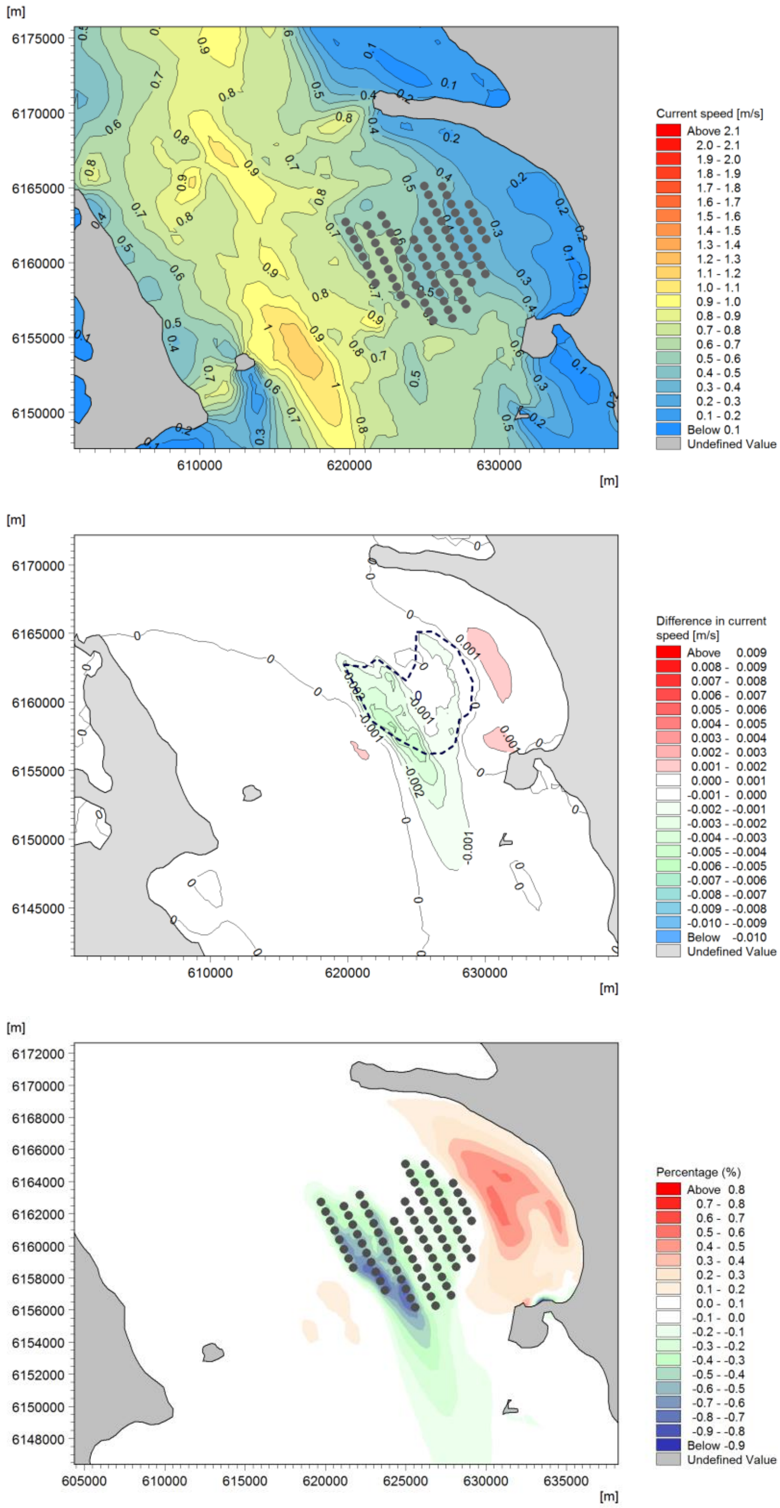

Figure 6.3. Simulated tidal current velocities in the bottom layer with the foundations in place (top panel). Bottom layer change in tidal current velocities (m/s) due to the foundation layout (middle panel) and percentage change relative to the baseline (bottom panel).

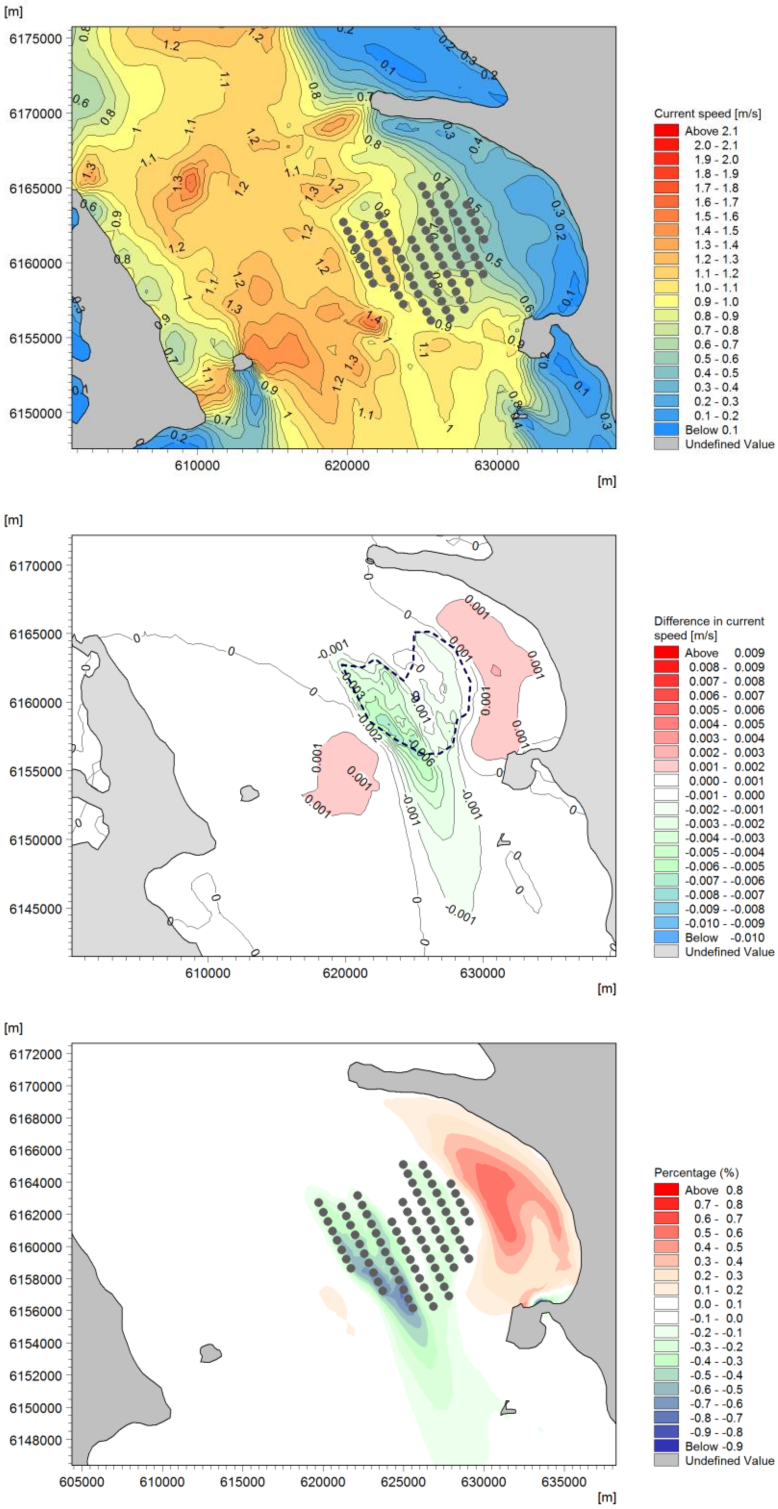

Figure 6.4. Simulated tidal current velocities in the middle layer with the foundations in place (top panel). Middle layer change in tidal current velocities (m/s) due to the foundation layout (middle panel) and percentage change relative to the baseline (bottom panel).

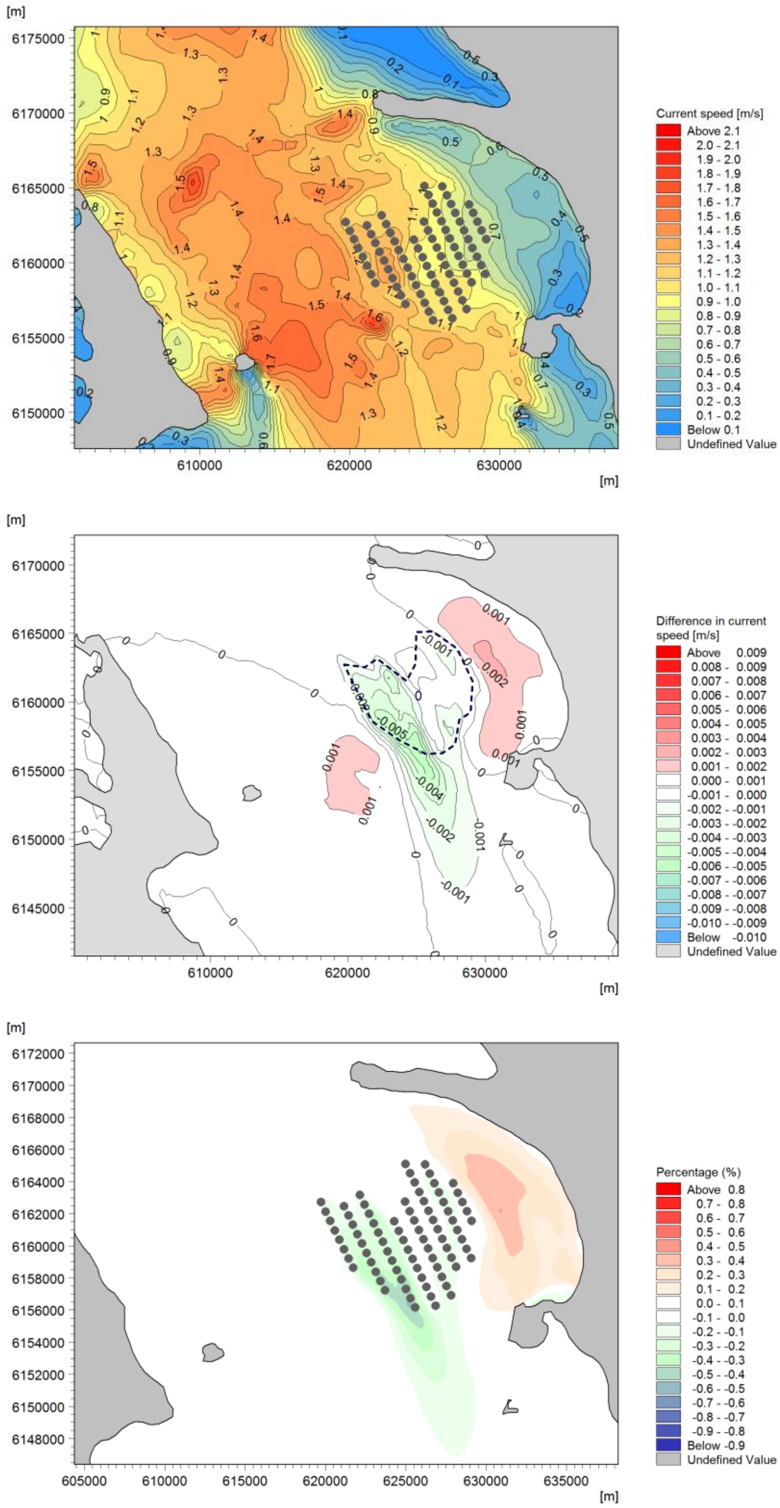

Figure 6.5. Simulated tidal current velocities in the surface layer with the foundations in place (top panel). Surface layer change in tidal current velocities (m/s) due to the foundation layout (middle panel) and percentage change relative to the baseline (bottom panel).

6.2. Pressures on Natura 2000 Sites of the Operational Phase

Due to the limited magnitude of change of hydrography caused by operation of the wind farm and export cable, the Magnitude of Pressure is considered to be low.

7. POTENTIAL PRESSURES DURING DECOMMISSIONING

The lifetime of the wind farm is expected to be around 25 years. Prior to expiry of the production time a decommissioning plan should be submitted. Currently, the decommissioning approach has not been defined, and therefore this assessment of potential pressures uses a worst case scenario of full removal of foundations, cables, turbine components and ancillary structures.

7.1. Foundations and Cables

The effects are likely to include short-term increases in suspended sediment concentration and sediment deposition from the plume caused by foundation cutting or dredging and seabed disturbance caused by removal of cables and cable protection. Limited impacts on water quality are anticipated as the sediments are not contaminated. Although there is no evidence base on these potential effects, the effects during decommissioning of the foundations, inter-array cables and export cables are considered to be less than those described during the construction phase. This is because there will be no need for seabed preparation and there is a possibility that cables are left *in situ* with no consequential increase in suspended sediment concentration or changes to water quality. As a result, the Magnitude of Pressure of changes to hydrography, sediment spill and water quality caused by decommissioning of Jammerland Bight is considered to be low.

7.2. Removal of Turbine Components and Ancillary Structures

During decommissioning of both the turbine components and ancillary structures, all fluids and substances will need to be removed. The effects during decommissioning are considered to be similar to those described during the construction phase; hence, the Magnitude of Pressure is considered to be low.

8. CUMULATIVE PRESSURES

The assessment of cumulative effects evaluates the extent of the environmental effects of Jammerland Bight in terms of intensity and geographic extent compared with other projects in the area. The assessment of the cumulative conditions includes activities associated with existing utilised and un-utilised permits or approved plans for projects. When projects within the same region affect the same environmental conditions simultaneously, they are defined to have cumulative impacts. Given that there are no developments within the vicinity of Jammerland Bight, there are no cumulative effects.

9. IMPACT ASSESSMENT SUMMARY

9.1. Impacts on Natura 2000 Sites

Due to the limited, local and temporary magnitude of change to hydrography and sediment spill caused by construction, operation and decommissioning of the wind farm, the degree of impact is predicted to be low. Due to the designated status of the potential receptors, the importance is assessed as very high and so the resulting severity of the impact is predicted to be low. Overall, due to the relatively small effects in terms of scale, no impact is predicted (Table 9.1).

Table 9.1. Summary of impact assessment for water quality related to Natura 2000 sites.

Parameter	Construction	Operation	Decommissioning
Magnitude of Pressure	Low	Low	Low
Sensitivity	Medium	Medium	Medium
Degree of Impact	Low	Low	Low
Importance	Very High	Very High	Very High
Severity of Impact	Low	Low	Low
Overall Impact Significance	No Impact	No Impact	No Impact

9.2. Impacts on Suspended Sediment Concentrations and Deposition

The degree of impact is predicted to be low for both suspended sediment in the water column and sediment deposition from the plume for both the construction and decommissioning of the wind farm. In order to determine the severity of impact, the importance of the receptor has to be considered. Based on the descriptions provided in Sections 1.4 and 1.6, an importance level of medium has been defined, since changes to suspended sediment concentrations in the water column and variations in sediment deposition rates are important for local ecosystem functioning. The resulting severity of the impact is therefore low. Overall, the significance of the impact is considered to be negligible negative since the impacts are localised, short term and will revert to baseline conditions following cessation of the activities (Table 9.2).

Table 9.2. Summary of impact assessment for suspended sediment concentrations and deposition for the foundations, inter-array and export cables.

Parameter	Construction	Decommissioning
Magnitude of Pressure	Low	Low
Sensitivity	Medium	Medium
Degree of Impact	Low	Low
Importance	Medium	Medium
Severity of Impact	Low	Low
Overall Impact Significance	Negligible Negative	Negligible Negative

9.3. Impacts on Tidal Currents

The degree of impact is predicted to be low for tidal currents during operation of the wind farm. In order to determine the severity of impact, the importance of the receptor has to be considered. Based on the descriptions provided in Section 1.5, an importance level of medium has been defined, since changes to tidal current velocities may result in changes to sediment transport patterns both offshore and at the coast. The resulting severity of the impact is therefore low. Since the very small changes to tidal current velocities caused by the foundations will not affect sediment transport over and above the natural baseline processes, no impact is predicted (Table 9.3).

Table 9.3. Summary of impact assessment for tidal current velocities and wave heights during operation of the foundations.

Parameter	Operation
	Tidal Currents
Magnitude of Pressure	Low
Sensitivity	Low
Degree of Impact	Low
Importance	Medium
Severity of Impact	Low
Overall Impact Significance	No Impact

10. REFERENCES

Energinet.dk. (2013). *Technical Project Description for the Large-scale Offshore Wind Farm (400 MW) at Horns Rev 3*, March 2013.

Energinet.dk. (2014). *Horns Rev 3 Offshore Wind Farm Technical report no. 3: Hydrography, Sediment Spill, Water Quality, Geomorphology and Coastal Morphology*, April 2014.

Forewind. (2013). *Dogger Bank Creyke Beck Offshore Wind Farm Environmental Statement*. Chapter 9 Marine Physical Processes.

DHI. (2014a). *DHI MIKE3 Flow Model – Scientific Documentation and User Guide*.

DHI. (2014b). *DHI MIKE3 Mud Transport Module – User Guide*.

Orbicon. (2014). *Horns Rev 3 Offshore Wind Farm. Fish Ecology. Technical report no. 5*. Report to Energinet.dk.

APPENDIX A – MODEL CALIBRATION RESULTS

Regional Model Calibration Results

Figures A.1 and A.2 show the simulated water levels compared with the measurements for eight of the tidal stations around the Danish Baltic Sea coast. The measured water level data show the effects of wind set-up / wind set-down during the 6-7th December storm. Wind set-up occurs in the Kattegat while wind set-down occurs in the southern part connected to the Baltic sea. These characteristics are captured well by the regional model. The calibration results show that the model can simulate successfully the wind set-up at Grena, Juelsminde and Hornbæk, and the wind set-down at Drogden, Kolding and Gedser. At Fynshav and Bagenkop, the mode results seem to over-simulate the water level set down (by about 0.5-1m) during the extreme surge event.

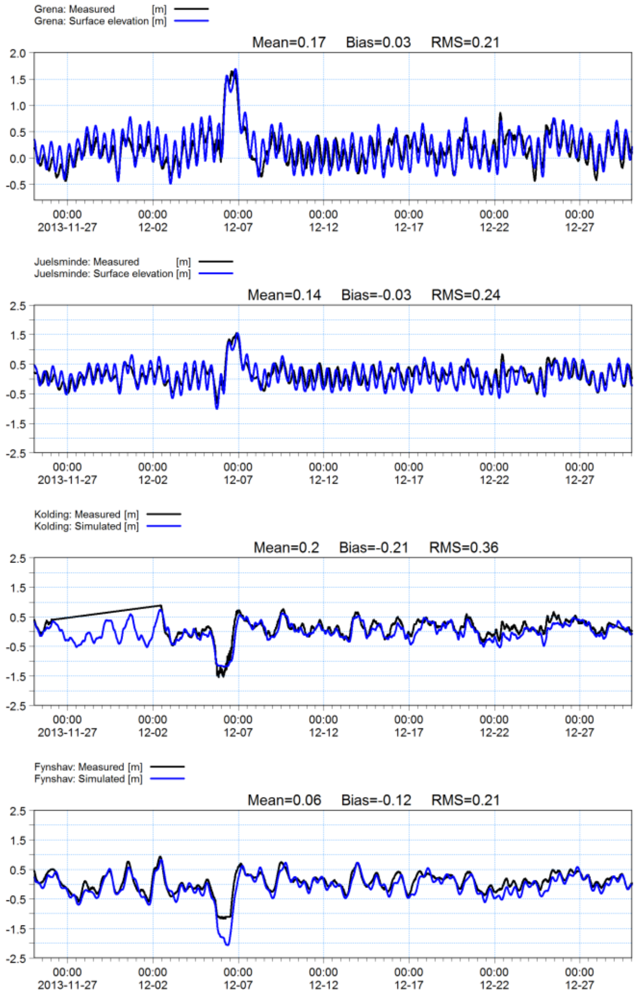

Figure A.1. Time series comparison between simulated (blue) and observed (black) water levels along the mainland Danish coast.

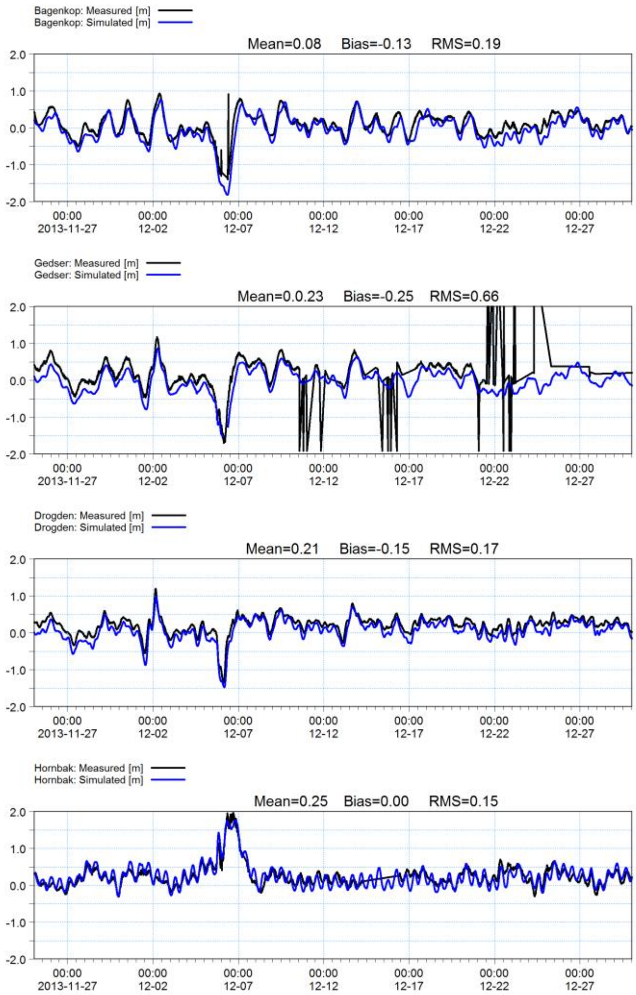

Figure A.2. Time series comparison between simulated (blue) and observed (black) water levels around the coasts of the Danish islands.

Statistical analyses were employed to quantify the model's water levels. The mean error, bias and root mean squared (RMS) error were computed for each station (Table A.1).

Table A.1. Summary of statistics for tidal current velocities

Nr.	Longitude	Latitude	Station name	Statistical parameters		
1	10,921962	56,412075	Grena	0.21	0.03	0.17
2	10,016333	55,71559	Juelsminde	0.24	-0.03	0.14
3	9,482401	55,489933	Kolding	0.36	-0.21	0.20
4	9,985632	54,994396	Fynshav	0.21	-0.12	0.06
5	10,6723585	54,751656	Bagenkop	0.19	-0.13	0.08
6	12,457139	56,09339	Hornbæk	0.15	0.00	0.25
7	12,711318	55,536377	Drogden	0.17	-0.15	0.21
8	11,924483	54,57212	Gedser	0.66	-0.25	0.23

In general, the mean error, bias and RMS errors are less than 0.25. This indicates a reasonable agreement between the observed and modelled results. Due to some gaps in the recorded data, the RMS errors at Kolding and Gedser are high (0.36 and 0.66, respectively). However, the observed and simulated tidal phases were approximately the same for all periods.

Overall, the calibration results indicate that the water levels are well predicted for most stations. The good calibration results in terms of water levels indicate that the regional 2D model is reasonable to derive the water level boundary conditions for local 3D model.

Local Model Calibration Results

The comparisons of tidal currents between measurement at the Østerrenden station and simulation are shown in Figures A.3 and A.4. The current velocities and directions are compared at depths of 5m, 10m and 14m relative to mean sea level from the sea surface downwards. The comparisons show reasonable agreement between measured and simulated current velocity during the early stages and during the extreme event (6-7th December) at all layers. The modelled current directions also matched well with the measurements. After the storm (8th December), the wind speed reduced significantly, from 26m/s to 5m/s and the wind direction turned rapidly from 320°N to 200°N. It appears that the model is unable to capture the rapid variation in the current directions for this period, resulting in underestimation of current velocities. During later stages, the model performed well for both current velocity and direction.

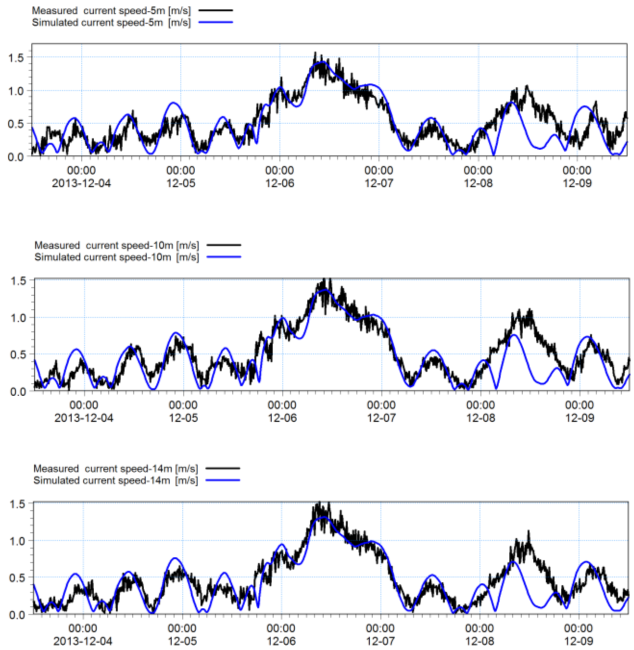

Figure A.3. Time series comparison between simulated (blue) and observed (black) current velocities at Østerrenden.

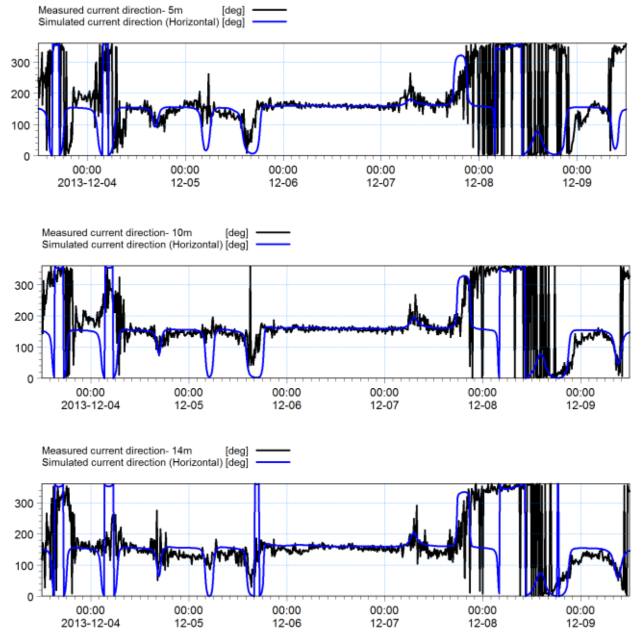

Figure A.4. Time series comparison between simulated (blue) and observed (black) current direction at Østerrenden.

The comparison between the two modelled tidal currents at Point 6 is presented in Figures A.5 to A.8. The comparison of tidal current velocity and direction shows that the two models perform similarly during extreme conditions. Figure A.7 presents tidal currents in u-v directions at 2m and 10m below mean sea level. The modelled results matched well with the DMI modelled data. The comparison of salinities and temperatures are shown in Figure A.8. The temperature and salinity variations are insignificant in vertical and horizontal dimensions over the simulated period. This may result from the weather changes due to the extreme storm conditions.

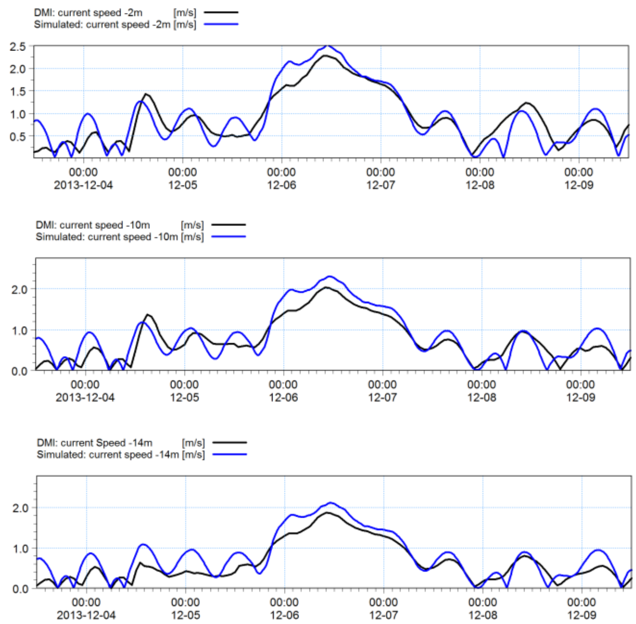

Figure A.5. Time series comparison between simulated (blue) and DMI modelled (black) current velocity at Point 6.

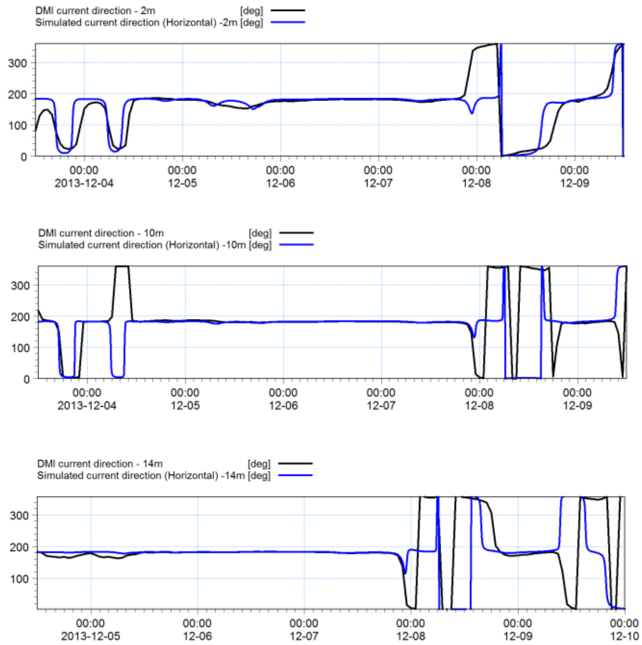

Figure A.6. Time series comparison between simulated (blue) and DMI modelled (black) current direction at Point 6.

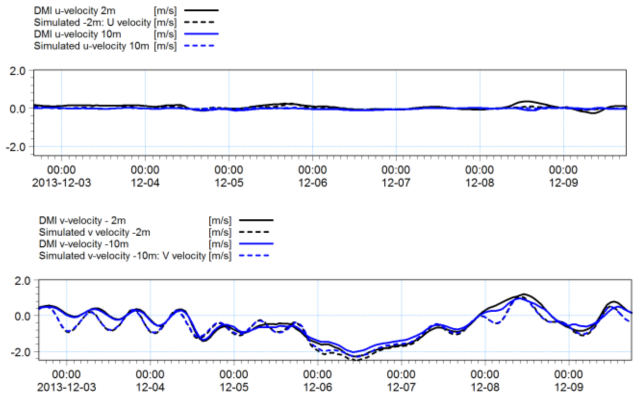

Figure A.7. Time series comparison between simulated (blue) and DMI modelled (black) current u-v direction at Point 6.

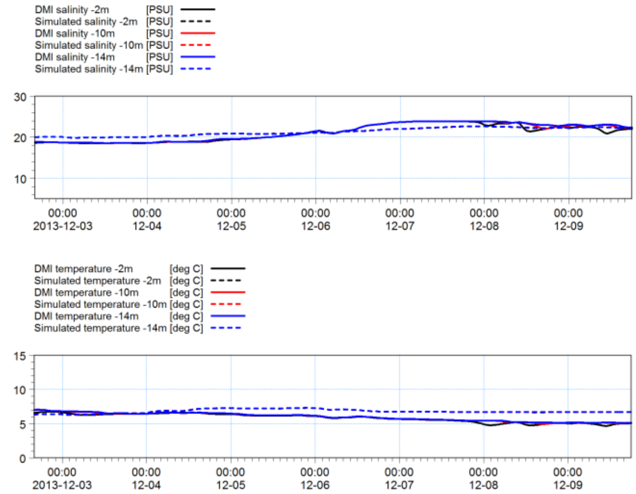

Figure A.8. Time series comparison between simulated (blue) and DMI modelled (black) salinity and temperature data at Point 6.

The modelled temperatures are higher/lower than the DMI modelled temperatures data by about 3ºC. The modelled salinity is higher than the DMI modelled salinities with a maximum difference of 3 PSU over the water depth at the end of the calibration period. The difference in both comparisons may be due to the differences in setting between two models. The 3D local model does not consider surface (2m) air temperature, surface air (2m) humidity and cloud cover while the DMI model included those inputs and activated heat exchange. The number of vertical layers for the computational meshes is also different. However, it is expected that the small difference in salinity and temperature do not affect the current patterns significantly.